2 In-plane loading – membrane elements

2.5 Compatibility and deformation capacity

This chapter examines the load-deformation behaviour of reinforced concrete membrane elements using the example of orthogonally reinforced membrane elements subjected to uniform in-plane loading. In particular, the *Cracked Membrane Model* (CMM) developed at ETH Zurich will be introduced. This mechanically consistent model enables a realistic investigation of the load-deformation behaviour.

The load-bearing and deformation behaviour of reinforced concrete membrane elements is generally quite complex. First, the basic features of the behaviour of membrane elements (not predominantly loaded in compression) are described. Afterwards, possible calculation models and solution methods for the behaviour of orthogonally reinforced membrane elements in the cracked state are discussed.

Learning objectives

Within this chapter, the students are able to:

- describe how using an effective compressive strength dependent on the transverse strain state modifies the boundaries of the membrane yield conditions.
- discuss the differences and similitudes between various compression field models which can be used to investigate the load-deformation behaviour of reinforced concrete membrane elements.
- formulate the main assumptions of the Cracked Membrane Model with stress-free cracks, including how to model tension stiffening for bidirectional reinforcement using the Tension Chord Model.

2 In-plane loading – membrane elements

2.5 Compatibility and deformation capacity

A) Influence of strains on the compressive strength and thus on the yield conditions

Membrane elements – Effective compressive strength

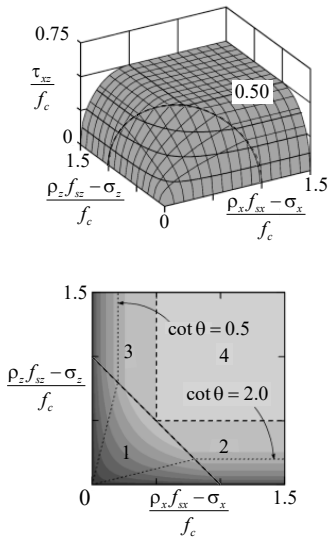

Constant concrete compressive strength
(f_c independent of ε_1)

On this and the following two slides (from Kaufmann (1998)) the influence of a *strain state dependent compressive strength* on the resistance of orthogonally reinforced membrane elements is investigated. Note that we also referred to this effect as *compression softening* when presenting this topic for the particular case of walls and beams.

The consideration of a compressive strength dependent on the strain state requires carrying out load-deformation analyses (see following section). However, the influence can be analytically approximated in some regions of the yield surface with a simplified estimation of the strain state in the region, similarly as already presented in the chapter “Compatibility and deformation capacity of walls and beams”. Detailed investigations with a refined model (*Cracked Membrane Model* CMM) that will be later presented in this chapter, confirm the validity of this simplification.

This slide shows the yield condition of an orthogonally reinforced membrane element, which was derived just from equilibrium considerations in the last chapter considering a constant compressive strength (f_c). However, it was not discussed what is the “right” value of the effective compressive strength to be considered. The area in which failure occurs due to yielding of the two reinforcements (Regime 1) is triangular (bounded by the yellow line).

Membrane elements – Effective compressive strength

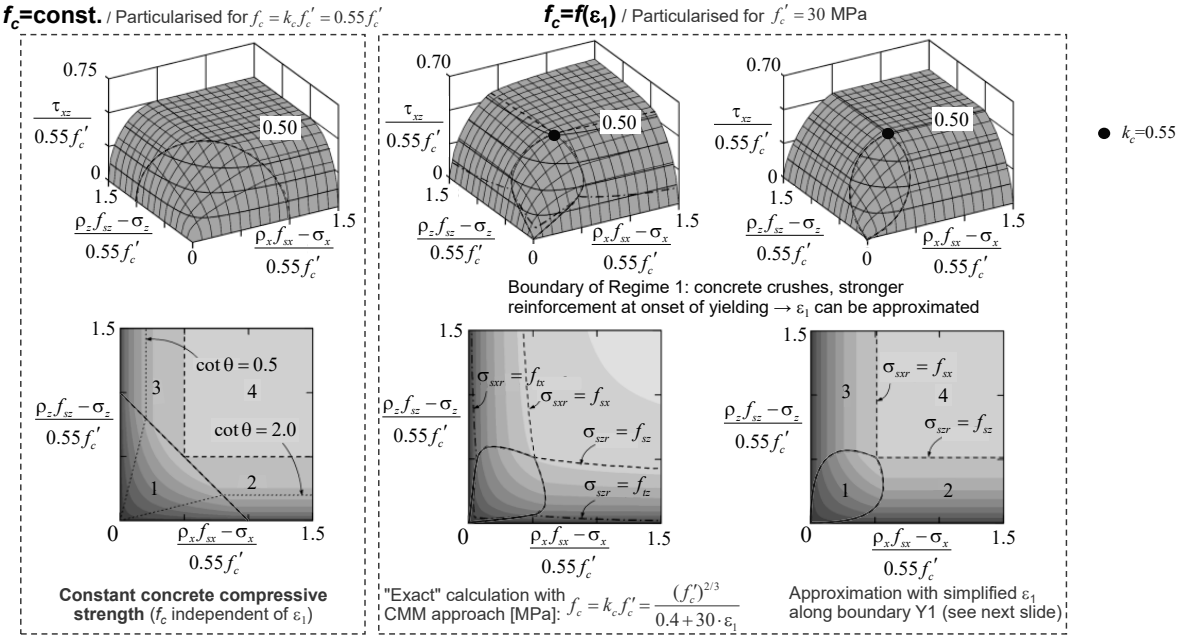

The figure on the left shows the yield condition for orthogonally reinforced membrane elements with constant compressive strength, shown in the last slide, but particularised for an effective compressive strength $f_c = f_{ce} = k_c \cdot f_c' = 0.55 \cdot f_c'$, where f_c' is the cylindrical compressive strength of concrete, which was also referred to as $f_{c,cyl}$ in the chapter of “Compatibility and deformation capacity of walls and beams”. The chosen effective compressive strength corresponds to the compressive strength typically considered for shear verifications in SIA 262 (i.e. $k_c = 0.55$).

The figure in the middle shows calculations with the CMM (tedious, each point of the diagram corresponds to a full nonlinear load-deformation analysis). The figure on the right shows the approximation presented on the next page, based on a simplified estimation of the strain field. This fits well with the more precise calculations.

It is important to note that a compressive strength dependent on the strain state has *no influence on the load-bearing resistance in Regime 1,* since the resistance in this Regime is uniquely determined by the yielding of the two reinforcements. However, it does influence the boundaries of Regime 1 and the resistance in Regimes 2, 3, etc.

The area in which failure occurs due to yielding of the two reinforcements (Regime 1) is triangular when considering a constant compressive strength (left graph). With a compressive strength dependent on the strain state (lower compressive strength at large transverse tensile strains), early concrete failure occurs with very flat (or steep) stress field inclinations. Since the transverse strains are larger with such inclinations, the area of Regime 1 is therefore narrower in this case.

The transition point between Regimes 1, 2 and 3 has the same effective compressive strength in all three cases ($f_c = f_{ce} = k_c \cdot f_c' = 0.55 \cdot f_c'$). This effective compressive strength can be easily derived from the compression softening proposed by Kaufmann (1998) and a simplified estimation of the strain field, as shown in the following slide.

Membrane elements – Effective compressive strength

Influence on yield conditions

The yield surface can be modified by taking into account the dependence of the concrete compressive strength on the transverse strains.

→ Area of Regime 1 is reduced (affected: zones with very flat / steep inclinations)

→ Calculation with Cracked Membrane Model (CMM, middle graph) is tedious

→ Approximate solution (bottom graphs):

assuming: $k_c f_c' = \dfrac{(f_c')^{2/3}}{0.4 + 30 \cdot \varepsilon_1}$ (1998):

Y_1: $\tau_{xz}^2 = (\rho_x f_{sx} - \sigma_x)(\rho_z f_{sz} - \sigma_z)$ (unchanged)

Y_2: $\tau_{xz}^2 = (\rho_z f_{sz} - \sigma_z)^2 \left\{ \sqrt{2.0 + \dfrac{25}{3} \dfrac{(f_c')^{2/3}}{(\rho_z f_{sz} - \sigma_z)}} - \dfrac{29}{12} \right\}$

Y_3: $\tau_{xz}^2 = (\rho_x f_{sdx} - \sigma_x)^2 \left\{ \sqrt{2.0 + \dfrac{25}{3} \dfrac{(f_c')^{2/3}}{(\rho_x f_{sx} - \sigma_x)}} - \dfrac{29}{12} \right\}$

Y_4: $\tau_{xz}^2 = \left\{ \dfrac{25}{29} (f_c')^{2/3} \right\}^2$

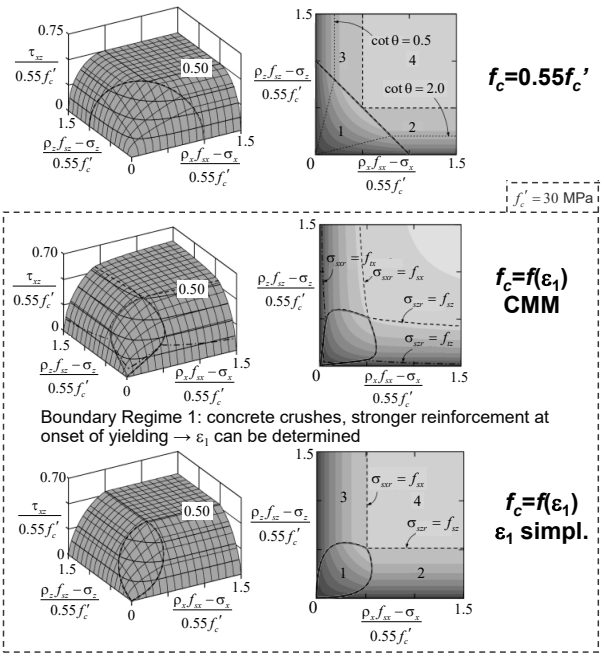

On the right side, the yield conditions for ideally plastic behaviour and constant concrete compressive strength $0.55 \cdot f_c'$ is shown in the top figure. The failure conditions considering the deformation-dependency of the concrete compressive strength are shown below it (same figures as on the previous slide).

The approximated approach (bottom figures) is based on the assumptions that the concrete compression is $\varepsilon_3 = -\varepsilon_{cu} = -0.002$ at the boundary of Regime 1 and the stronger reinforcement just reaches the yield point, in which tension stiffening is accounted for with a simplified factor of 0.8 ($\varepsilon_{sm} = 0.8 \cdot f_s / E_s = 0.8 \cdot 500/200'000 = 0.002$).

Thus, the principal tensile strain ε_1 follows at the boundary between Regimes 1 and 2 with $\varepsilon_3 = -\varepsilon_{cu}$ and $\varepsilon_x = \varepsilon_{sm}$ from the relationship $\varepsilon_1 = \varepsilon_x + (\varepsilon_x - \varepsilon_3)\cot^2\alpha$, since the compression field inclination α is known. At the Regime boundary, both reinforcements just yield when the concrete crushes:

$$\cot^2 \alpha = (a_{sx} f_{sx} - n_x) / (a_{sz} f_{sz} - n_z)$$

By inserting this into the following equation for the effective concrete compressive strength, the equations presented in the slide are obtained:

$$k_c f_c' = \frac{(f_c')^{2/3}}{0.4 + 30 \cdot \varepsilon_1}$$

For the Regime 1 boundary these equations agree very well (since the assumptions made apply to the strains at the Regime 1 boundary). For areas further away, the approximation is still generally sufficient.

Derivation of k_c = 0.55 with approximated approach (transition point Regimes 1, 2 and 3)*:*

α = 45°; $\varepsilon_3 = -0.002$; $\varepsilon_x = 0.002$

$\varepsilon_1 = \varepsilon_x + (\varepsilon_x - \varepsilon_3)\cot^2\alpha = 0.006$

$$k_c f_c' = \frac{(f_c')^{2/3}}{0.4 + 30 \cdot \varepsilon_1} = 1.72 (f_c')^{2/3} \rightarrow k_c = 1.72 (f_c')^{-1/3} \xrightarrow{f_c' = 30 \text{ MPa}} k_c = 0.55$$ (characteristic value in SIA 262)

Membrane elements – Effective compressive strength

Influence on yield conditions

The yield surface can be modified by taking into account the dependence of the concrete compressive strength on the transverse strains.

→ Area of Regime 1 is reduced (affected: zones with very flat / steep inclinations)

→ Calculation with Cracked Membrane Model (CMM, middle graph) is tedious

→ Approximate solution (bottom graphs):

according to SIA: (2013), $k_c f_c = \frac{f_c}{1.2 + 55 \cdot \varepsilon_1}$:

Y_1: $\tau_{xz}^2 = (\rho_x f_{sdx} - \sigma_x)(\rho_z f_{sdz} - \sigma_z)$ (unchanged)

Y_2: $\tau_{xz}^2 = (\rho_z f_{sdz} - \sigma_z)^2 \left\{ \sqrt{\frac{135}{22} + \frac{50}{11} \frac{f_c}{(\rho_z f_{sdz} - \sigma_z)}} - \frac{73}{21} \right\}$

Y_3: $\tau_{xz}^2 = (\rho_x f_{sdx} - \sigma_x)^2 \left\{ \sqrt{\frac{135}{22} + \frac{50}{11} \frac{f_c}{(\rho_x f_{sdx} - \sigma_x)}} - \frac{73}{21} \right\}$

Y_4: $\tau_{xz}^2 = \left\{ \frac{16}{49} f_c \right\}^2$ (d.h. $\tau_{xz} = 0.327 \cdot f_c \approx \frac{0.65 \cdot f_c}{2}$)

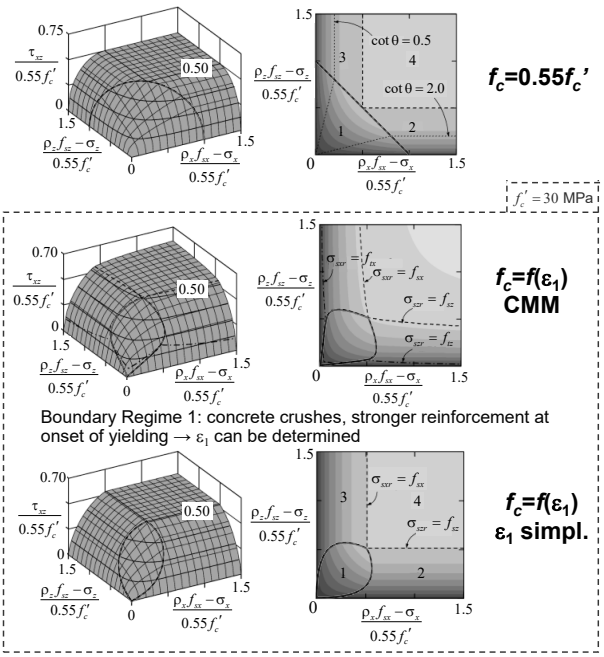

f_c=0.55f_c'

f_c=f(ε_1) CMM

f_c=f(ε_1) ε_1 simpl.

The equations shown on the previous page apply to the relationship for the effective concrete compressive strength according to Kaufmann (1998).

Following the same procedure, the approximate solution can also be derived for the effective concrete compressive strength according to the standard SIA 262 (see slide). These equations can also be used for a fully code-compliant design in Regimes 2, 3, and 4.

Note that the nomenclature of this slide has been changed with respect to the previous ones in order to be more consistent with the original formulation contained in SIA 262. In this case, f_c denotes the reference cylindrical compressive strength, which in the previous slides was referred to as f_c' *or* $f_{c,cyl}$.

Derivation of k_c in the transition point Regimes 1, 2, and 3*:*

α = 45°; $\varepsilon_3 = -0.002$; $\varepsilon_x = 0.002$

$\varepsilon_1 = \varepsilon_x + (\varepsilon_x - \varepsilon_3)\cot^2\alpha = 0.006$

$k_c f_c' = \frac{f_c'}{1.2 + 55 \cdot \varepsilon_1} = 0.65 f_c' \rightarrow k_c = 0.65$

2 In-plane loading – membrane elements

2.5 Compatibility and deformation capacity

B) Load-deformation behaviour of membranes

Membrane elements - Load-deformation behaviour

General

Experiment VN2
V = 360 kN
$\alpha_r \approx 30°$

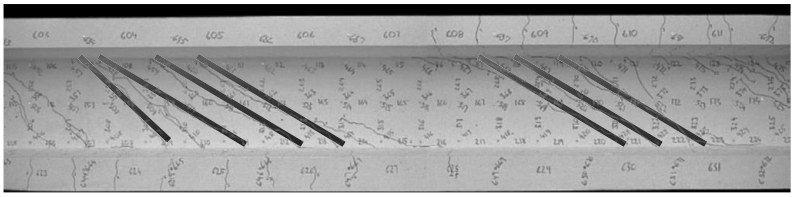

Experiment VN2
V = 545 kN
$\alpha_r \approx 17…25°$

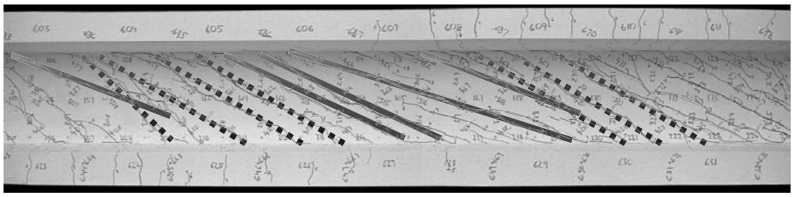

Experiment VN2
V = 548 kN
(failure)

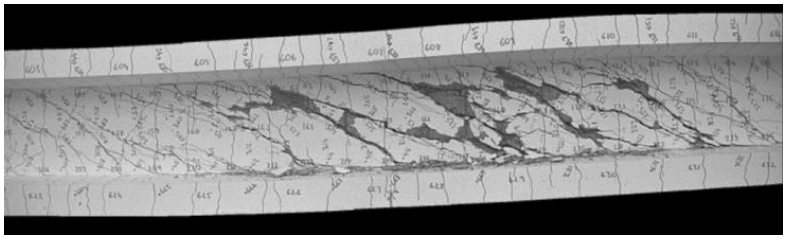

Before cracking, the behaviour differs only slightly from that of a homogeneous concrete membrane element, with the exception of residual stresses caused by the shrinkage of the concrete, which is restrained by the reinforcement. If the principal tensile stress in the concrete exceeds the tensile strength, cracks form approximately perpendicular to the principal tensile stress direction. Crack formation is associated with the redistribution of internal forces, which generally leads to a change in the principal stress directions immediately after crack formation. If sufficient minimum reinforcement is present, the reinforcement is initially elastically stressed after crack formation. In this case, the principal stress directions remain approximately constant after cracking, until the membrane element fails due to the crushing of the concrete (over-reinforced elements, should be avoided) or the stresses in one of the two reinforcements (i.e. longitudinal or transverse) exceed the yield strength.

Since the stiffness of the reinforcement drops considerably after the onset of yielding, further redistributions of forces take place. As the load increases, new cracks appear which, in comparison with the previous cracks, run closer to the direction of the non-yielding reinforcement. When the load is further increased, the membrane element finally fails due to the crushing of the concrete or due to the yielding of the previously elastic reinforcement. In the latter case, both longitudinal and transverse reinforcements yield during failure, resulting in a very ductile failure behaviour. However, if the concrete crushes before both reinforcements yield or if the weaker reinforcement ruptures already during crack formation (or before the stronger reinforcement yields), a more brittle behaviour must be expected.

The figure illustrates the behaviour using the cracks in a beam under "pure shear" (constant shear force, moment equal to zero at midspan): The cracks in the web become flatter with increasing load.

Membrane elements - Load-deformation behaviour

General

Experiment MVN1
V = 210 kN
$\alpha_r \approx$ 35...55°

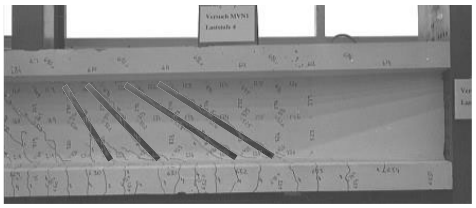

Experiment MVN1
V = 510 kN
$\alpha_r \approx 25°$

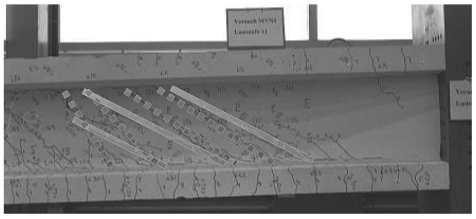

Experiment MVN1
V = 540 kN
(failure)

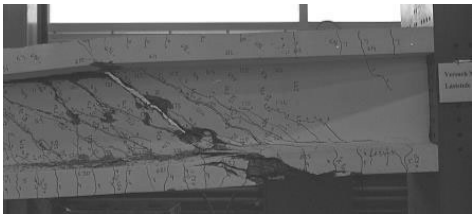

During the loading process, generally, cracks with different directions form. The cracks that do not run in the principal concrete stress direction must obviously transfer shear stresses, which theoretically could lead to failure by sliding along the cracks. However, tests have shown that (at least in conventional concrete) the aggregate interlock is usually sufficient to transmit the shear stresses, such that sliding along cracks only occurs in exceptional cases.

The figure illustrates the behaviour using the cracks in a beam under bending and transverse force: The cracks in the web become flatter with increasing load.

Membrane elements - Load-deformation behaviour

Reinforced concrete membrane element under monotonous load increase

1. Uncracked behaviour: Like homogeneous concrete membrane element (slight differences due to restraint shrinkage etc.)
2. Initial cracking approximately perpendicular to the principal tensile stress direction
3. Crack formation → Redistribution of internal forces → Change of principal stress directions immediately after crack formation
4. Cracked-elastic behaviour: Principal stress directions ± constant as long as both reinforcements remain elastic
5. Yielding of a reinforcement
   → Decrease in stiffness → Further redistribution of internal forces
   → New cracks (closer to the direction of the non-yielding reinforcement)
6. Failure due to crushing of the concrete or yielding of the other reinforcement (possibly reinforcement ruptures or aggregate interlock fails)

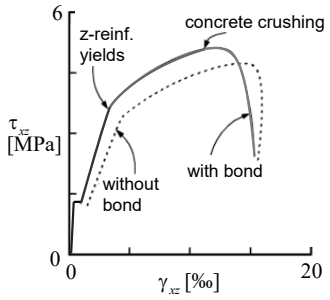

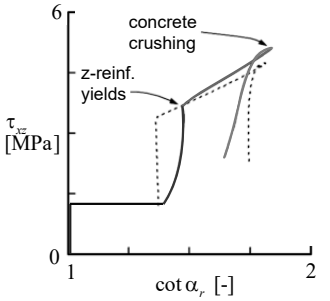

The figures on the right show the behaviour of an orthogonally reinforced membrane element under monotonously increasing, uniform shear stress (without normal membrane (in-plane) forces). The element is heavily reinforced in the *x*-direction, whereas in the *z*-direction, it has only weak reinforcement. The calculations were performed with the Cracked Membrane Model (CMM).

It can be seen that the principal stress direction changes abruptly at crack formation (principal stress direction becomes "flatter", i.e. it rotates in the direction of the stronger reinforcement). It then remains approximately constant until the weaker reinforcement yields. After the start of yielding of the weaker reinforcement, the principal stress direction becomes significantly flatter again, until in this example, the failure occurs due to crushing of the concrete.

The influence of the tension stiffening effect of the concrete between the cracks can also be clearly seen (without tension stiffening: dashed line). Since the concrete compressive strength depends on the strains (which decrease due to tension stiffening), the tension stiffening also increases the load capacity (if the failure does not occur due to the yielding of both reinforcements, i.e. in Regime 1, where the ultimate load is independent of the concrete strength).

Additional remark:

With very flat compression field inclinations (weak reinforcement in *z*-direction), large strains occur, in particular also in the vertical direction. Since the weak *z*-reinforcement has a relatively stiff bond (thin bars), in such cases, the failure often occurs due to rupture of the *z*-reinforcement. It is also possible that a failure may occur due to the failure of aggregate interlock in the steeper cracks from earlier load stages (which must transmit large forces but have wide crack openings).

Membrane elements - Load-deformation behaviour

Test facilities for uniformly stressed elements

Shear Panel Tester
University of Toronto 1979

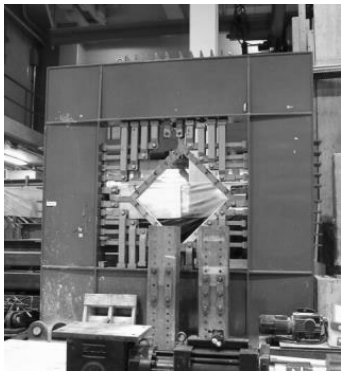

Shell Element Tester
University of Toronto 1984 / 2009

Large Universal Shell Element Tester
ETH Zürich 2017

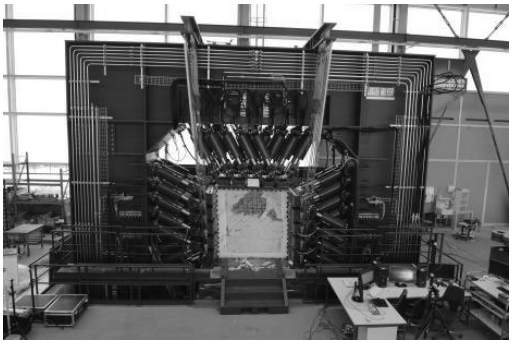

The behaviour of reinforced concrete membrane elements under uniform membrane (in-plane) loading can be investigated in special test facilities. This slide shows three test facilities with which large-scale elements of reinforced concrete membrane elements can be tested under uniform loading:

- *Shear Panel Tester* of the University of Toronto
  developed by Prof. Vecchio, 1979

- *Shell Element Tester* of the University of Toronto
  developed by Prof. Marti + Prof. Collins 1984
  Upgrade to servo hydraulics by Prof. Collins + Prof. Bentz 2009

- *Large Universal Shell Element Tester (LUSET)* from ETH Zurich
  developed by Prof. Kaufmann 2017

It is no coincidence that two of the facilities are located at the University of Toronto, one of the world's leading universities in reinforced concrete design. Like ETH Zurich, it has excellent facilities for large-scale experiments and a long tradition of carrying them out. A fourth facility is located at the University of Houston ("Universal Element Tester", essentially a copy of the Shell Element Tester with slightly smaller dimensions, elements approx. 1‘397x1‘397x400 mm).

Today these are the only test facilities in the world with which large-scale elements of reinforced concrete membrane elements can be tested under uniform membrane loading (a few years ago there was another facility for membrane loading in Japan (Kajima Corp.), but it no longer exists).

Large Universal Shell Element Tester LUSET, ETH Zurich (2017)

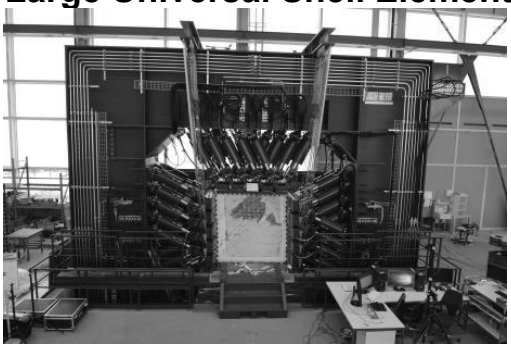

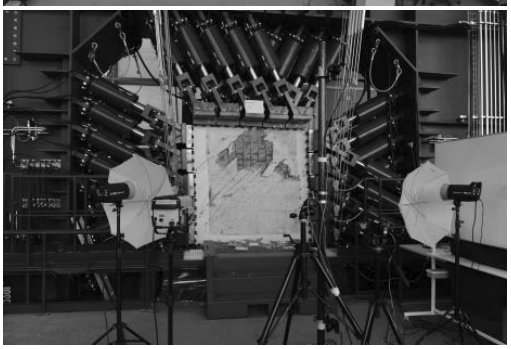

General loading (8 stress resultants)

Applied loads in-plane and out-of-plane of general direction, i.e. perpendicular and parallel to element edge

→ principal direction of applied loads variable

→ reinforcing bars parallel to element edges

Element size 2,000-2,000-350 mm

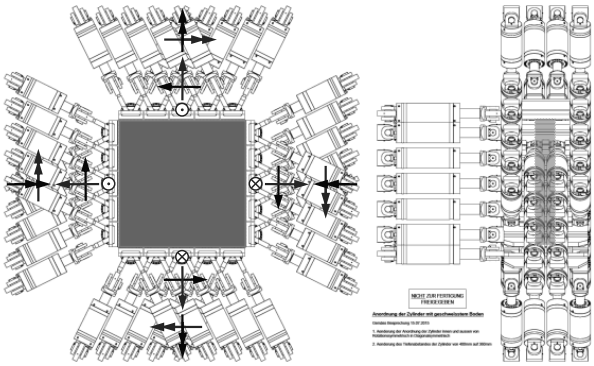

In the *Large Universal Shell Element Tester* (LUSET), elements with dimensions of 2,000x2,000x350 mm can be tested under general shell loading (8 stress resultant elements): membrane (in-plane) forces $\{n_x, n_z, n_{xz}\}$, bending and twisting moments $\{m_x, m_z, m_{xz}\}$, and transverse (out-of-plane) shear forces $\{v_x, v_z\}$).

In contrast to the Shell Element Tester in Toronto, the principal direction of the applied membrane stress is variable. LUSET thus combines the advantages of the Shear Panel Tester (membrane stress with variable principal direction) and the Shell Element Tester (general stress due to 8 stress resultants, large dimensions of the elements).

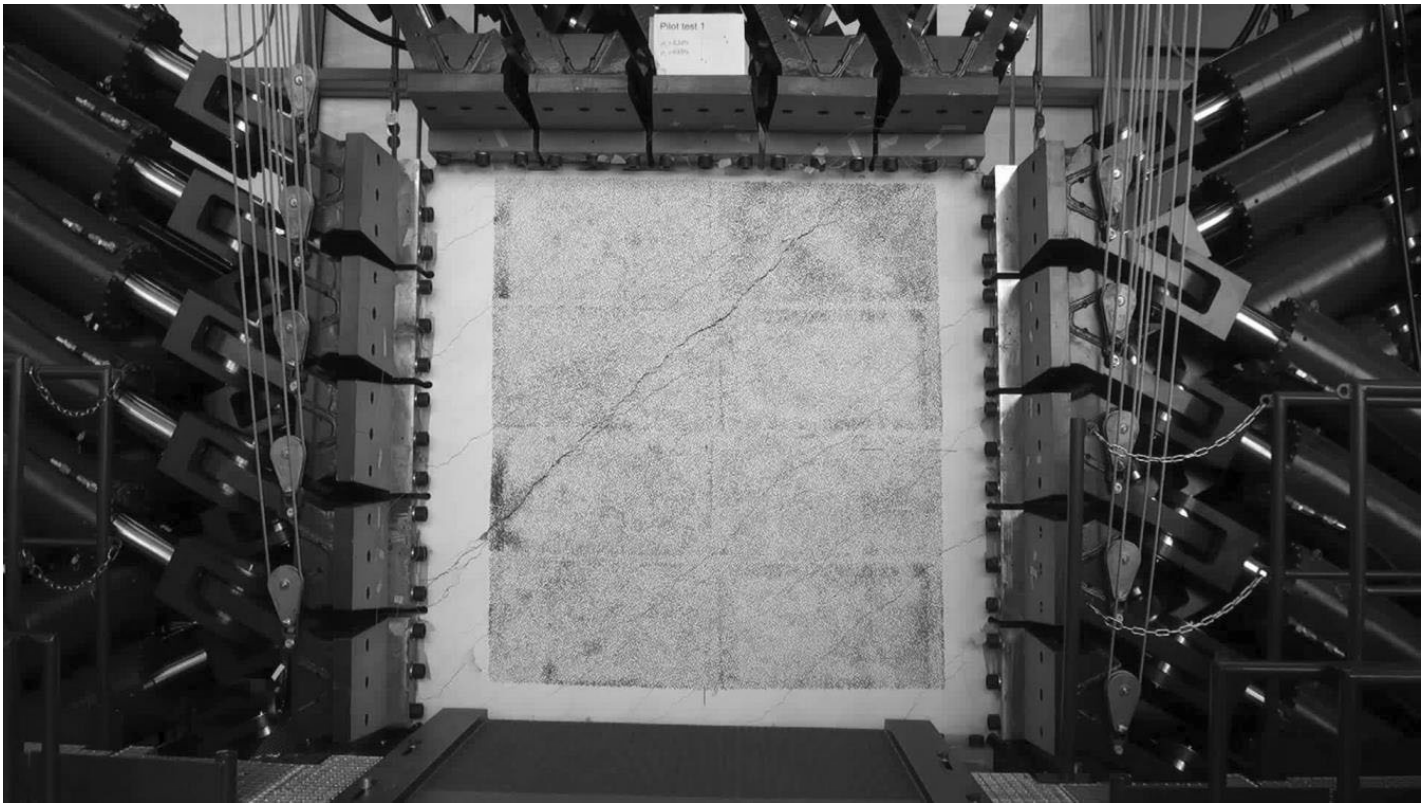
Pilot test 1

2 In-plane loading – membrane elements

2.5 Compatibility and deformation capacity

C) Compression field approaches

Membrane elements - Load-deformation behaviour

External loads are in equilibrium with reinforced concrete = concrete + reinforcing steel

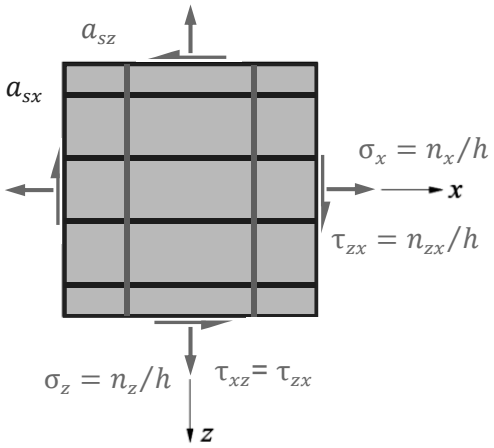

Equilibrium of forces [kN/m]

$$n_x = n_{xc} + n_{xs} = n_{xc} + a_{sx}\sigma_{sx}$$
$$n_z = n_{zc} + n_{zs} = n_{xc} + a_{sz}\sigma_{sz}$$
$$n_{xz} = n_{xzc} + \cancel{n_{xzs}} = n_{xzc}$$

Orthogonal reinforcement (dowelling action is neglected)

Equilibrium in equivalent stresses [MPa]

$$\sigma_x = \sigma_{xc} + \rho_x\sigma_{sx}$$
$$\sigma_z = \sigma_{zc} + \rho_z\sigma_{sz}$$
$$\tau_{xz} = \tau_{xzc}$$

(with $\rho_x\sigma_{sx}$, $\rho_z\sigma_{sz}$ = stresses in the reinforcement, $\rho_x = a_{sx}/h$, $\rho_z = a_{sz}/h$)

Repetition from Stahlbeton I:

The applied load $\{n_x, n_z, n_{xz}\} = h \cdot \{\sigma_x, \sigma_z, \tau_{xz}\}$ corresponds to the sum of the forces in the concrete $\{n_x, n_z, n_{xz}\}_c = h \cdot \{\sigma_{xc}, \sigma_{zc}, \tau_{xzc}\}$ and in the reinforcement $\{n_{xs}, n_{zs}, 0\} = h \cdot \{\rho_x\sigma_{sx}, \rho_z\sigma_z, 0\}$, where $n_{xzs} = 0$ applies to orthogonal reinforcement (only forces in bar direction).

Membrane elements - Load-deformation behaviour

External loads are in equilibrium with reinforced concrete = concrete + reinforcing steel

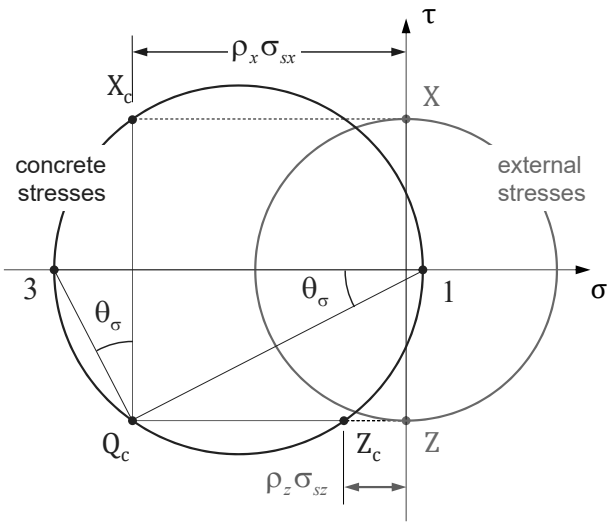

Equilibrium of forces [kN/m]

$$n_x = n_{xc} + n_{xs} \qquad = n_{xc} + a_{sx}\sigma_{sx}$$
$$n_z = n_{zc} + n_{zs} \qquad = n_{xc} + a_{sz}\sigma_{sz}$$
$$n_{xz} = n_{xzc} \qquad = n_{xzc}$$

Equilibrium in equivalent stresses [MPa]

$$\sigma_x = \sigma_{c3}\cos^2\theta_\sigma + \sigma_{c1}\sin^2\theta_\sigma + \rho_x\sigma_{sx}$$
$$\sigma_z = \sigma_{c3}\sin^2\theta_\sigma + \sigma_{c1}\cos^2\theta_\sigma + \rho_z\sigma_{sz}$$
$$\tau_{xz} = (\sigma_{c1} - \sigma_{c3})\sin\theta_\sigma\cos\theta_\sigma$$

(with $\rho_x\sigma_{sx}$, $\rho_z\sigma_{sz}$ = stresses in the reinforcement, $\rho_x = a_{sx}/h$, $\rho_z = a_{sz}/h$)

Membrane elements - Load-deformation behaviour

External loads are in equilibrium with reinforced concrete = concrete + reinforcing steel

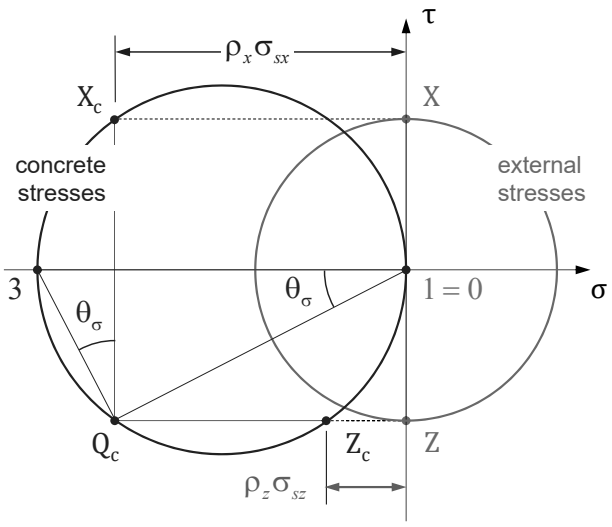

Equilibrium of forces [kN/m]

$$n_x = n_{xc} + n_{xs} \qquad = n_{xc} + a_{sx}\sigma_{sx}$$
$$n_z = n_{zc} + n_{zs} \qquad = n_{xc} + a_{sz}\sigma_{sz}$$
$$n_{xz} = n_{xzc} \qquad = n_{xzc}$$

Equilibrium in equivalent stresses [MPa]

$$\sigma_x = \sigma_{c3}\cos^2\theta_\sigma + \cancel{\sigma_{c1}\sin^2\theta_\sigma} + \rho_x\sigma_{sx}$$
$$\sigma_z = \sigma_{c3}\sin^2\theta_\sigma + \cancel{\sigma_{c1}\cos^2\theta_\sigma} + \rho_z\sigma_{sz}$$
$$\tau_{xz} = \cancel{(\sigma_{c1} - \sigma_{c3})}\sin\theta_\sigma\cos\theta_\sigma$$

$\sigma_{c1} = 0$ (uniaxial compression in concrete, i.e. stress-free cracks with variable direction)

(with $\rho_x\sigma_{sx}$, $\rho_z\sigma_{sz}$ = stresses in the reinforcement, $\rho_x = a_{sx}/h$, $\rho_z = a_{sz}/h$)

Membrane elements - Load-deformation behaviour

Compatibility - Mohr's strain circle

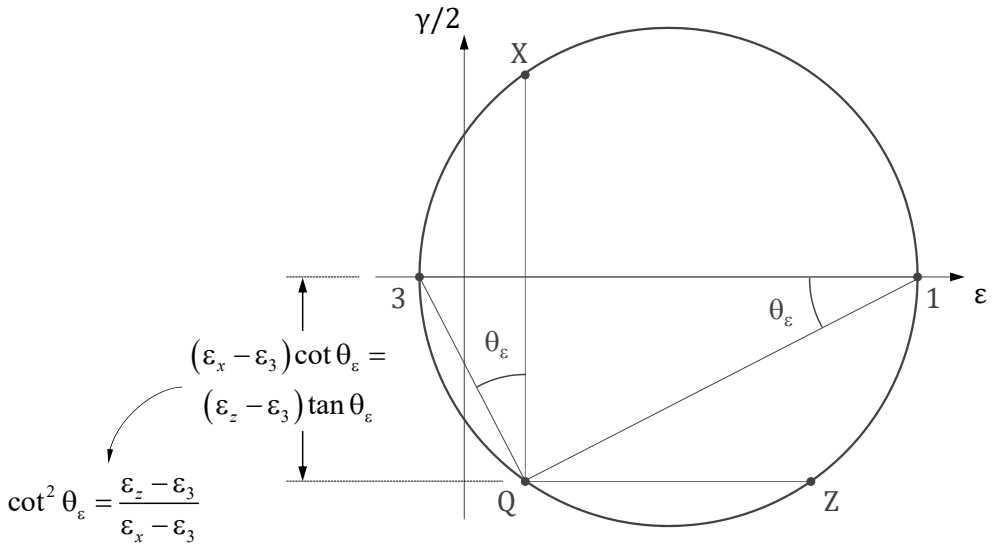

Each compatible strain state can be described by 3 non-collinear strains (3 unknowns).

Strains in cracked membrane elements

Total strains {ε} = strains in concrete between cracks {ε}$^{(c)}$ + average strains due to crack kinematics {ε}$^{(r)}$

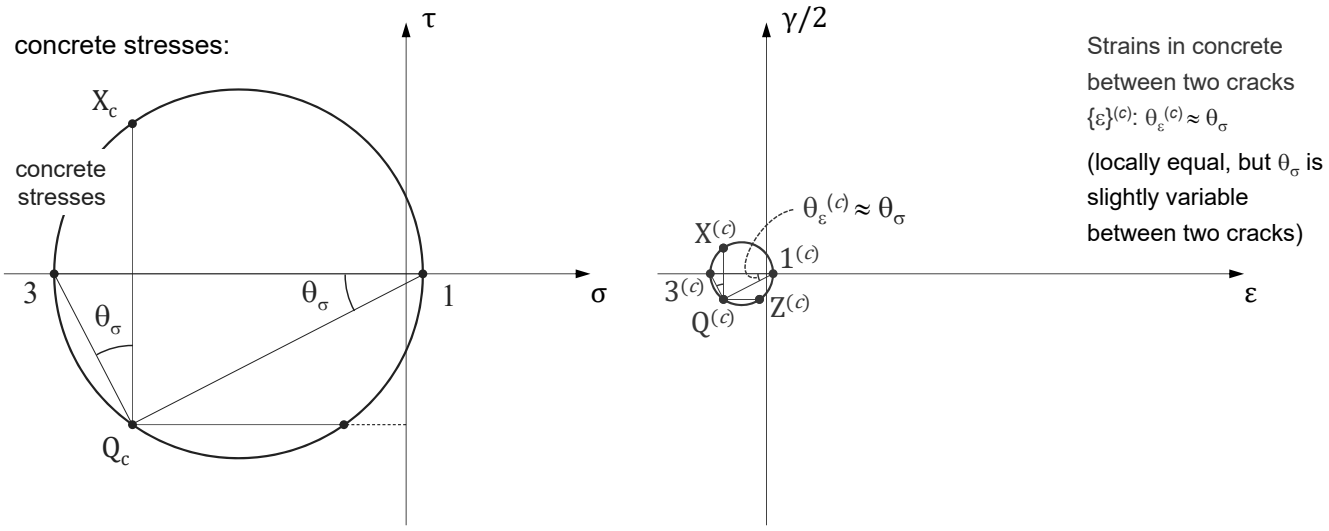

The total strains in the cracked-elastic state II are composed of the strains in the concrete between the cracks and the strains due to crack kinematics. The strains of the concrete can be determined from the concrete stresses using the material constitutive relationship.

Strains in cracked membrane elements

Total strains $\{\varepsilon\}$ = strains in concrete between cracks $\{\varepsilon\}^{(c)}$ + average strains due to crack kinematics $\{\varepsilon\}^{(r)}$

Concrete strains $\{\varepsilon\}^{(c)}$ between two cracks (local variation along *u*):

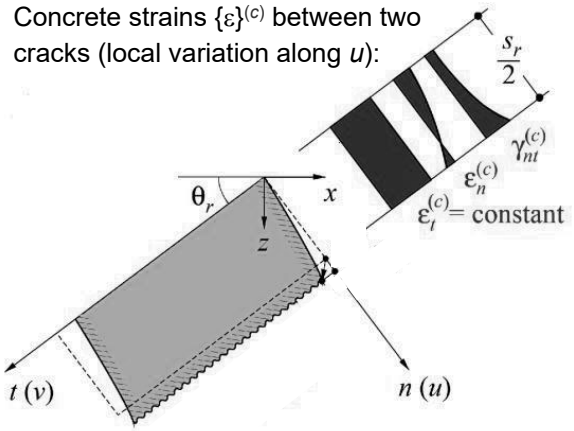

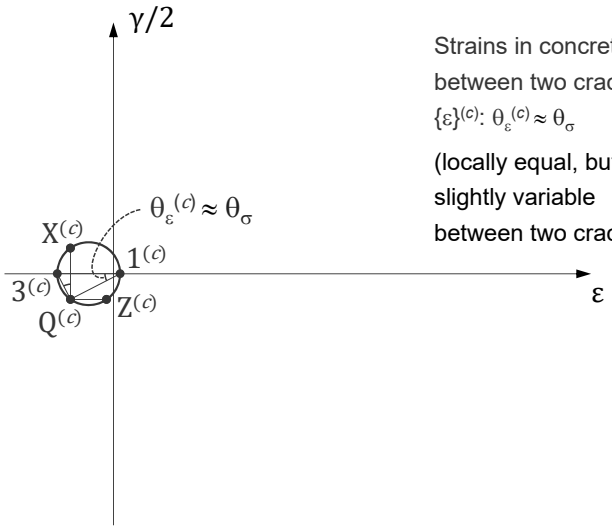

Strains in concrete between two cracks $\{\varepsilon\}^{(c)}$: $\theta_\varepsilon{}^{(c)} \approx \theta_\sigma$

(locally equal, but θ_σ is slightly variable between two cracks)

The strains in the concrete vary locally between the cracks along the *n*-axis (along the *t*-axis they are constant). Since this variation is very small, the strains of the concrete are often averaged over the crack spacing. Thus, a computationally less complex solution method can be used.

Strains in cracked membrane elements

Total strains $\{\varepsilon\}$ = strains in concrete between cracks $\{\varepsilon\}^{(c)}$ + average strains due to crack kinematics $\{\varepsilon\}^{(r)}$

Crack kinematics (parallel set of cracks):

s_r crack spacing
θ_r crack inclination
n, t coordinates $\perp$ and // to the crack

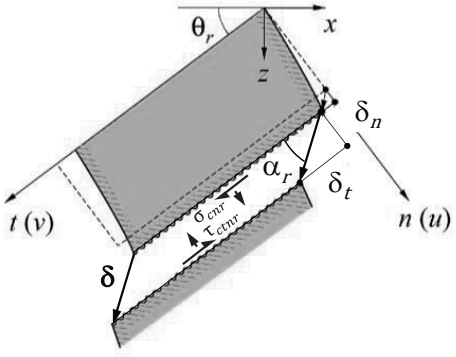

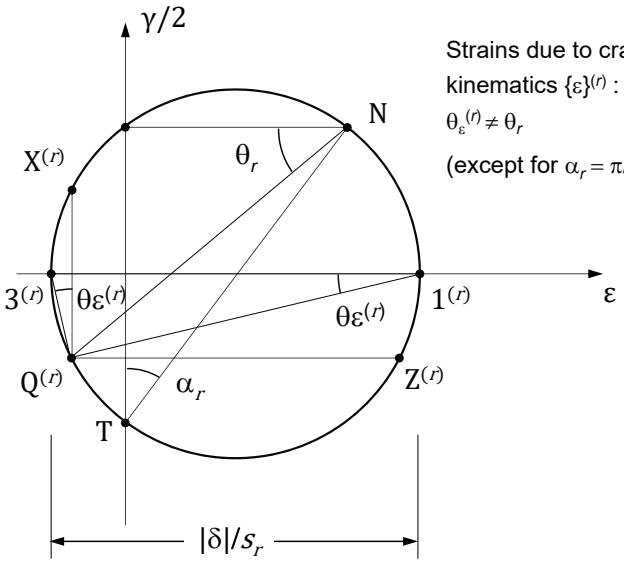

Strains due to crack kinematics $\{\varepsilon\}^{(r)}$:
$\theta_\varepsilon{}^{(r)} \neq \theta_r$
(except for $\alpha_r = \pi/2$)

The average strains due to crack kinematics are determined from the crack edge displacements δ_n and δ_t, by "smearing" them over the crack spacing s_r .

Strains in cracked membrane elements

Total strains $\{\varepsilon\}$ = strains in concrete between cracks $\{\varepsilon\}^{(c)}$ + average strains due to crack kinematics $\{\varepsilon\}^{(r)}$

Contribution to total strain:

- $\{\varepsilon\}^{(c)}$ (average along s_r)
- $\{\varepsilon\}^{(r)}$ (smeared along s_r)

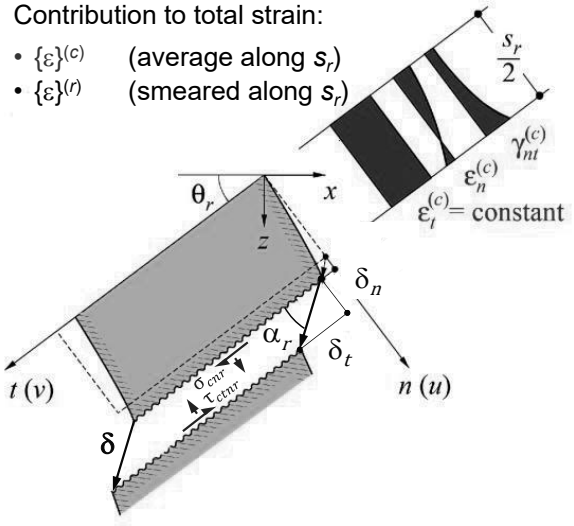

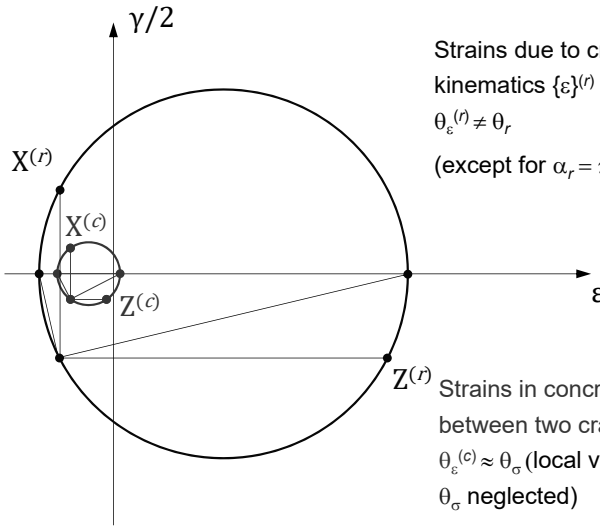

Strains due to crack kinematics $\{\varepsilon\}^{(r)}$:
$\theta_\varepsilon{}^{(r)} \neq \theta_r$
(except for $\alpha_r = \pi/2$)

Strains in concrete between two cracks $\{\varepsilon\}^{(c)}$:
$\theta_\varepsilon{}^{(c)} \approx \theta_\sigma$ (local variation of θ_σ neglected)

The strains in the concrete between the cracks are typically much smaller than the average strains due to crack kinematics.

Strains in cracked membrane elements

Total strains {ε} = strains in concrete between cracks {ε}$^{(c)}$ + average strains due to crack kinematics {ε}$^{(r)}$

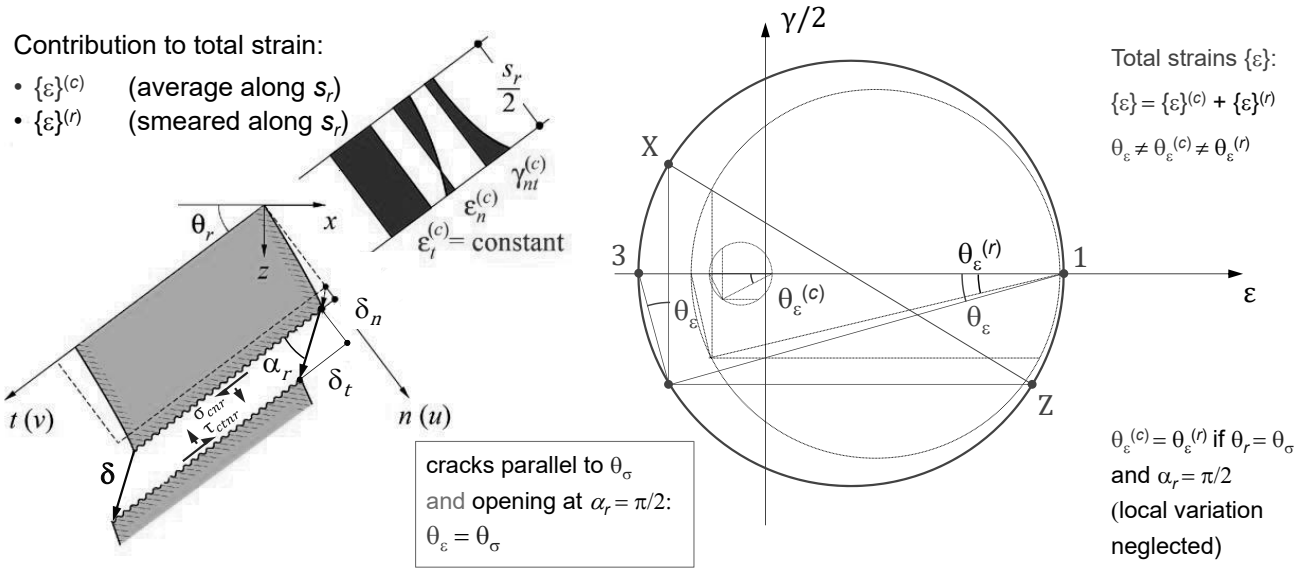

The total strains can be determined from the superposition of the average strains of the concrete between the cracks and the average strains due to crack kinematics. The two Mohr's circles can be graphically superimposed directly (summation of the components (ε_x, $\gamma_{xz}/2$) or (ε_z, $\gamma_{xz}/2$) in the *x* or *z* direction).

Compression field models

	Classic compression field model	Modified compression field theory (MCFT)	Cracked membrane model with rotating cracks (CMM-R)	Cracked membrane model with fixed cracks (CMM-F)
Main assumptions	Stress-free rotating cracks $\theta_\sigma = \theta_\varepsilon = \theta_r$ $\sigma_{c1} = 0$	"Stress-free" rotating cracks $\theta_\sigma = \theta_\varepsilon = \theta_r$ $\sigma_{c1/m}(\varepsilon_1) > 0$ (avg. tension stiff.)	Stress-free rotating cracks $\theta_\sigma = \theta_\varepsilon = \theta_r$ $\sigma_{c1/r} = 0$	Fixed interlocked cracks $\theta_{\sigma r} \neq \theta_\varepsilon \neq \theta_r$ $\sigma_{c1/r} \neq 0$ (aggregate interlock)
Equilibrium	(3 equations)	in average stresses (3 equations)	at the crack (3 equations)	at the cracks (7 equations)
Compression softening	neglected (ultimate load overestimated)	considered	considered	considered
Tension stiffening	neglected (stiffness underestimated)	as average concrete property (lack of consistency)	according to tension chord model	according to tension chord model
Crack spacing	$s_r \rightarrow 0$	s_r can**not** be estimated	s_r can be estimated	s_r can be estimated
Deformation capacity	**cannot** be estimated	**cannot** be consistently estimated	**can** be estimated	**can** be estimated

The load-deformation behaviour of reinforced concrete membrane elements can be investigated with *compression field models.* Such models are characterised by the fact that the load-bearing behaviour is dominated by a compressive stress condition in the concrete that is inclined in relation to the reinforcement directions. Smaller tensile or compressive stresses in the concrete may act perpendicular to these principal compressive stresses. Models, which consider interlocked cracks of given, fixed inclination, can also be called *compression field models*.

This slide gives an overview of the most relevant *compression field models*, which are discussed in detail in the following slides and the annex.

Compression field models

Classic compression field model with $f_{ct} = 0$ – stress-free cracks with variable crack inclination

Equilibrium

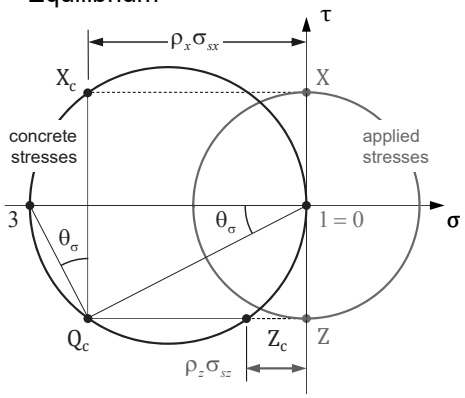

$$\sigma_x = \sigma_{c3} \cos^2 \theta_\sigma + \rho_x \sigma_{sx}$$
$$\sigma_z = \sigma_{c3} \sin^2 \theta_\sigma + \rho_z \sigma_{sz}$$
$$\tau_{xz} = -\sigma_{c3} \sin \theta_\sigma \cos \theta_\sigma$$

Compatibility

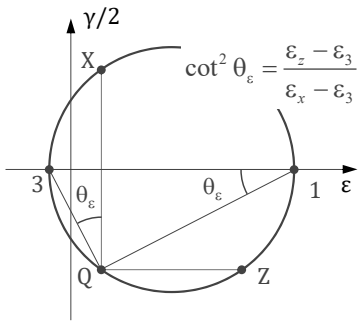

cracks parallel to θ_σ
and opening at $\alpha_r = \pi/2$
$\rightarrow \theta_\varepsilon = \theta_\sigma$

Material properties

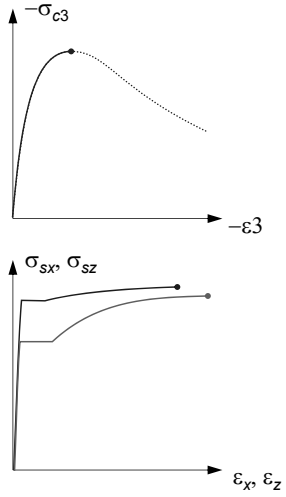

According to the classical compression field model, fictitious, rotating cracks with infinitesimally small crack spacing are considered (see figure). These cracks are stress-free, run parallel to the principal compressive stress direction and open perpendicularly to their direction. The principal directions of the stresses and strains are therefore identical. Variations of the stresses in the reinforcement and in the concrete (especially due to bond) are neglected. A uniform uniaxial compressive stress condition therefore prevails in the concrete. The principal directions can adjust during the load history depending on the magnitude of the applied loads. In general, the principal directions rotate with increasing load.

The strain state is clearly determined by three arbitrary, non-collinear strains (see Mohr's circle), for example $\{\varepsilon_x, \varepsilon_z, \varepsilon_3\}$. If the constitutive relationships of concrete and reinforcement are known, all quantities in the three equilibrium equations can be expressed as a function of the three strains. With a given strain state, the stress state $\{\sigma_x, \sigma_z, \tau_{zx}\}$ can thus be determined by integration. Conversely, the determination of the strain state for a given stress usually requires an iterative procedure.

Compression field models

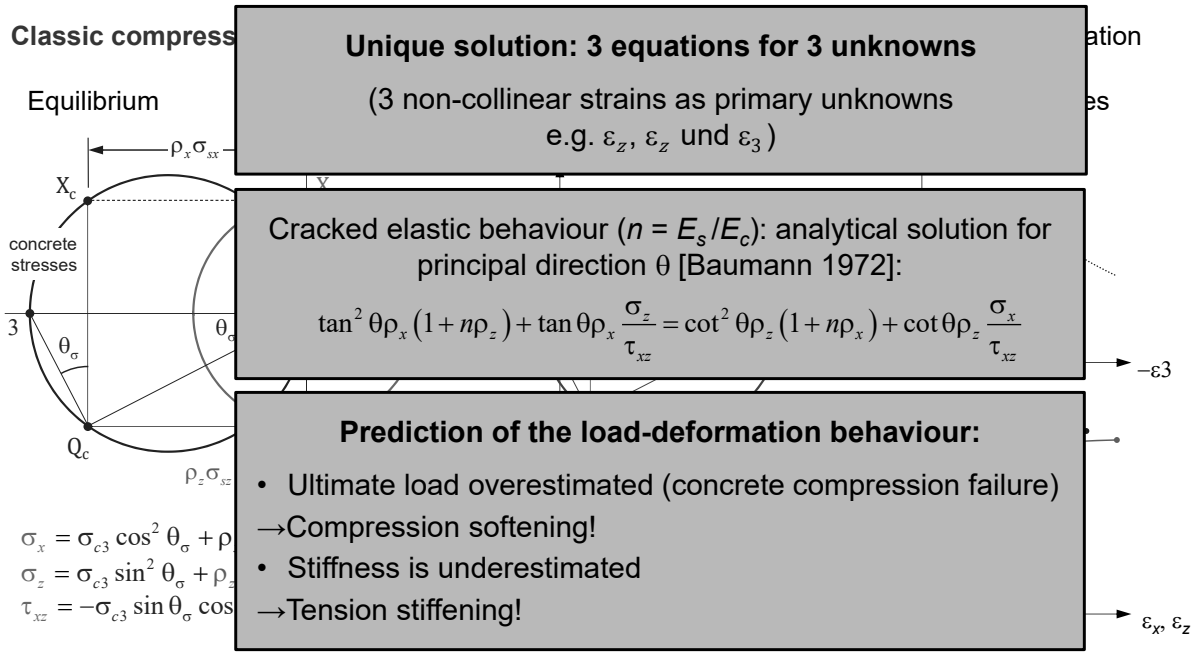

With classical compression field models, the deformations are greatly overestimated because rotating cracks are considered and the stiffening effect of the concrete between the cracks is neglected. Since the concrete compressive strength depends on the strain state ("compression softening"), the failure load can only be predicted inaccurately (except in under-reinforced elements whose failure occurs due to the yielding of both reinforcements).

The Kupfer-Baumann equation can be derived directly from the equilibrium and kinematic compatibility conditions assuming a cracked elastic behaviour.

Equilibrium

$$\sigma_x = \sigma_{c3}\cdot\cos(\theta)^2 + \sigma_{c1}\cdot\sin(\theta)^2 + \rho_x\cdot\sigma_{sx} \quad \rightarrow \quad \rho_x\cdot\sigma_{sx} = \sigma_x + \tau_{zx}\cdot\cot(\theta)$$

$$\sigma_z = \sigma_{c3}\cdot\sin(\theta)^2 + \sigma_{c1}\cdot\cos(\theta)^2 + \rho_z\cdot\sigma_{sz} \quad \rightarrow \quad \rho_z\cdot\sigma_{sz} = \sigma_z + \tau_{zx}\cdot\tan(\theta)$$

$$\tau_{zx} = (\sigma_{c1}-\sigma_{c3})\cdot\sin(\theta)\cdot\cos(\theta) \quad \rightarrow \quad \sigma_{c3} = -\tau_{zx}\cdot(\tan(\theta)+\cot(\theta))$$

Linear elasticity

$$\sigma_{sx} = E_s\cdot\varepsilon_x \quad \rightarrow \quad \varepsilon_x = \frac{\sigma_{sx}}{E_s} = \frac{\sigma_x + \tau_{zx}\cdot\cot(\theta)}{\rho_x\cdot E_s}$$

$$\sigma_{sz} = E_s\cdot\varepsilon_z \quad \rightarrow \quad \varepsilon_z = \frac{\sigma_{sz}}{E_s} = \frac{\sigma_z + \tau_{zx}\cdot\tan(\theta)}{\rho_z\cdot E_s}$$

$$\sigma_{c3} = \frac{E_s}{n}\cdot\varepsilon_3 \quad \rightarrow \quad \varepsilon_3 = \frac{n\cdot\sigma_{c3}}{E_s} = -\frac{n\cdot\left[\tau_{zx}\cdot(\tan(\theta)+\cot(\theta))\right]}{E_s}$$

Compatibility

$$\cot(\theta)^2 = \frac{\varepsilon_z-\varepsilon_3}{\varepsilon_x-\varepsilon_3} \quad \rightarrow \quad \cot(\theta)\cdot(\varepsilon_x-\varepsilon_3) = \tan(\theta)\cdot(\varepsilon_z-\varepsilon_3)$$

…

Compression field models

Modified compression field theory: Consideration of compression softening and tension stiffening

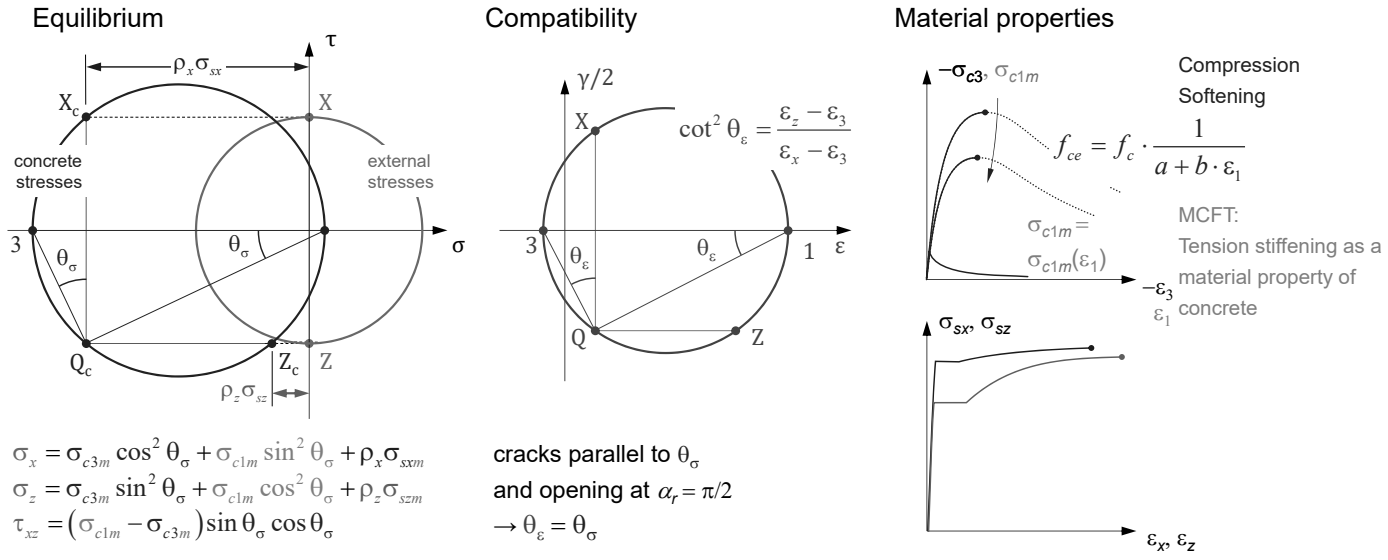

$$\sigma_x = \sigma_{c3m} \cos^2 \theta_\sigma + \sigma_{c1m} \sin^2 \theta_\sigma + \rho_x \sigma_{sxm}$$
$$\sigma_z = \sigma_{c3m} \sin^2 \theta_\sigma + \sigma_{c1m} \cos^2 \theta_\sigma + \rho_z \sigma_{szm}$$
$$\tau_{xz} = (\sigma_{c1m} - \sigma_{c3m}) \sin \theta_\sigma \cos \theta_\sigma$$

$$\cot^2 \theta_\varepsilon = \frac{\varepsilon_z - \varepsilon_3}{\varepsilon_x - \varepsilon_3}$$

$$f_{ce} = f_c \cdot \frac{1}{a + b \cdot \varepsilon_1}$$

$$\sigma_{c1m} = \sigma_{c1m}(\varepsilon_1)$$

In order to overcome the mentioned difficulties (too soft behaviour), various modifications of the classical compression field model were proposed.

The first of such models, the "Modified Compression Field Theory" proposed by Vecchio and Collins, is often used today. In this model, it is assumed that the principal directions of the strains and so-called average stresses in the concrete coincide. According to this model, the average principal concrete compressive stress is accompanied by an average principal concrete tensile stress. This has the consequence that the (average) steel stresses are lower than those according to the classical compression field model with equal stress and identical principal direction. Thus, the corresponding strains are lower, which equals an implicit consideration of bond. In the model, however, the stress-strain relationships of the bare steel are used as a function of average stresses and strains, which represents a conceptual weak point and leads to an overestimation of the load-bearing resistance (since tensile stresses in the concrete are acting simultaneously). To prevent this, an additional verification of the steel stresses at the cracks has been introduced, allowing considerable shear stresses on the crack faces. However, this is incompatible with the assumption underlying the model that the principal directions of average stresses and strains coincide.

The *Softened Truss Model*, which was later proposed by Hsu, is essentially the same as the *Modified Compression Field Theory.* However, it eliminates the conceptual weakness mentioned above by using appropriately adjusted relations for the average stresses in the reinforcement as a function of the mean strains (lowering the steel stresses to compensate for the concrete tensile stresses). However, this model was less successful.

Compression field models

Modified compression field theory: Consideration of compression softening and tension stiffening

Equilibrium | Compatibility | Material properties

Consideration of the tension stiffening by “average" tensile stresses in concrete (MCFT, Vecchio & Collins, 1986) leads to good overall results, but is not fully consistent:

- Overestimation of load capacity → verification "shear at crack" (incompatible with basic assumption $\theta_\varepsilon = \theta_\sigma$)
- There is no section with equilibrium in “average" stresses
- Tension stiffening ≠ Concrete property ≠ isotropic (main influence: ρ_x, $\rho_z \rightarrow$ orthotropic)
- No information on stresses at the crack, crack spacing, etc.

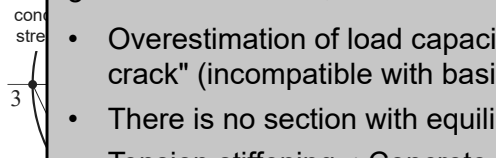

$$\sigma_x = \sigma_{c3m} \cos^2 \theta_\sigma + \sigma_{c1m} \sin^2 \theta_\sigma + \rho_x \sigma_{sxm}$$

$$\sigma_z = \sigma_{c3m} \sin^2 \theta_\sigma + \sigma_{c1m} \cos^2 \theta_\sigma + \rho_z \sigma_{szm}$$

$$\tau_{xz} = (\sigma_{c1m} - \sigma_{c3m}) \sin \theta_\sigma \cos \theta_\sigma$$

cracks parallel to θ_σ

and opening at $\alpha_r = \pi/2$

$\rightarrow \theta_\varepsilon = \theta_\sigma$

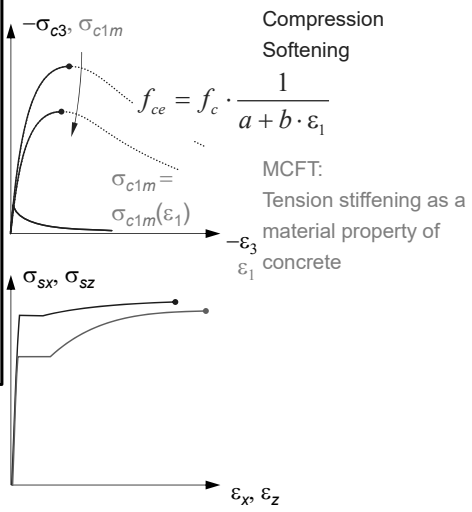

Compression Softening

MCFT: Tension stiffening as a material property of concrete

Compression field models

Cracked membrane model with rotating cracks: simplified

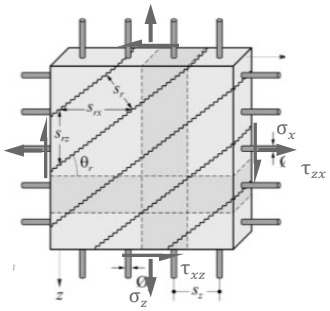

$$\sigma_{sxr} = \sigma_{sxr}(\varepsilon_x)$$
$$\sigma_{szr} = \sigma_{szr}(\varepsilon_z)$$

$$\sigma_x = \sigma_{c3r}\cos^2\theta_\sigma + \rho_x\sigma_{sxr}$$
$$\sigma_z = \sigma_{c3r}\sin^2\theta_\sigma + \rho_z\sigma_{szr}$$
$$\tau_{xz} = -\sigma_{c3r}\sin\theta_\sigma\cos\theta_\sigma$$

Assumption of stress-free cracks with variable crack direction

→ Stress field with uniaxial compression (parallel to crack direction) in concrete at cracks

Equilibrium at the crack

→ Equations identical to the classical compression field model with $f_{ct} = 0$

Treatment of reinforcement as tension chords

→ Tension stiffening increases stiffness, not ultimate load

→ Stress-strain relationships for stresses at crack σ_{sxr}, σ_{szr} with respect to mean strains ε_x, ε_z

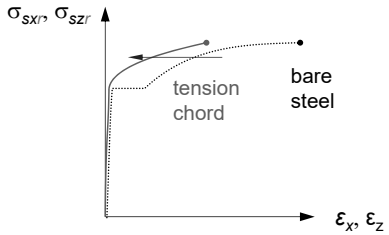

Neither the *Modified Compression Field Theory* nor the *Softened Truss Model* (or any other earlier compression field model) provides information about crack spacing, crack width, or the location of reinforcement strains near the crack. These models are therefore not suitable for investigating questions of minimum reinforcement or deformation capacity. In addition, models which formulate equilibrium as a function of average stresses between cracks have the disadvantage that by introducing average tensile stresses in the concrete, the connection to limit analysis is lost (there is no section on which equilibrium could be formulated in "average stresses"). Also for the investigation of the applicability of limit analysis (plasticity theory) methods, the discussed models are only suitable to a limited extent.

This unsatisfactory situation was the starting point for the development of the *Cracked Membrane Model (CMM*) at ETH Zurich in the late 1990s. This mechanically consistent model combines the concepts of the classical compression field model and the tension chord model. Crack spacing and tensile stresses between cracks are derived from basic principles of mechanics, and the link to the limit analysis for reinforced concrete membrane elements is maintained, since equilibrium is formulated in stresses at the cracks - and not in average stresses between the cracks.

In its general formulation (see below) the *Cracked Membrane Model* considers general crack inclinations, i.e. the cracks do not have to be stress-free or coincide with the principal strain directions. Following, the simplified CMM with stress-free cracks will be presented.

Compression field models

Cracked membrane model with rotating cracks: simplified

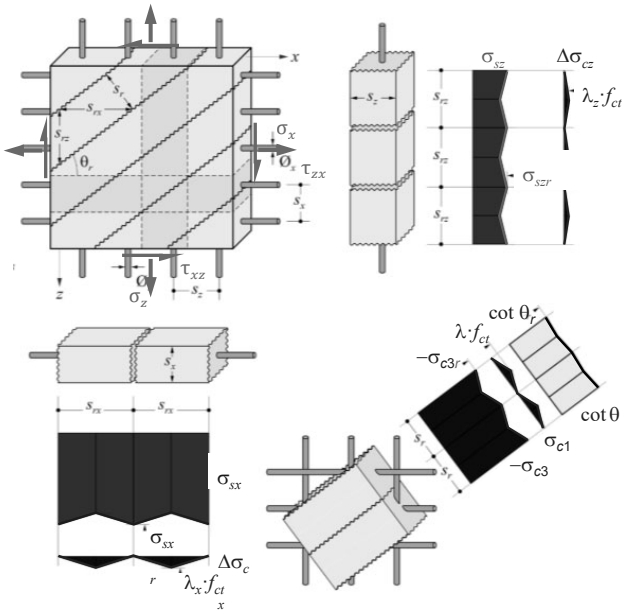

Assumption of stress-free cracks with variable crack direction

→ Stress field with uniaxial compression (parallel to crack direction) in concrete at cracks

Equilibrium at the crack

→ Equations identical to the classical compression field model with $f_{ct} = 0$

Treatment of reinforcement as tension chords

→ Tension stiffening increases stiffness, not ultimate load

→ Stress-strain relationships for stresses at crack σ_{sxr}, σ_{szr} as function of mean strains ε_x, ε_z

Determination of stresses in concrete and crack spacing

→ Stress in the concrete = superposition of the compression field and the stresses transferred to the concrete by bond

→ Condition for diagonal crack spacing: Principal tensile stress between two cracks must not exceed f_{ct}.

→ Crack spacings in the direction of reinforcement are geometrically linked to diagonal crack spacing:
$s_{rx} = s_r/\sin\theta_r$, $s_{rz} = s_r/\cos\theta_r$

Compression field models

Cracked membrane model with rotating cracks: Consideration of tension stiffening and compression softening

Equilibrium

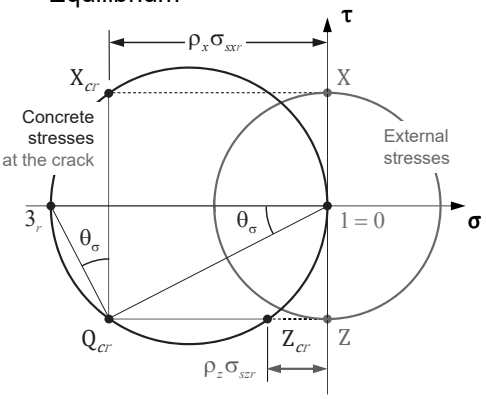

$$\sigma_x = \sigma_{c3r}\cos^2\theta_\sigma + \rho_x\sigma_{sxr}$$
$$\sigma_z = \sigma_{c3r}\sin^2\theta_\sigma + \rho_z\sigma_{szr}$$
$$\tau_{xz} = -\sigma_{c3r}\sin\theta_\sigma\cos\theta_\sigma$$

Compatibility

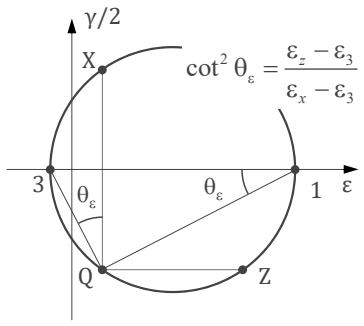

cracks parallel to θ_σ
and opening at $\alpha_r = \pi/2$
$\rightarrow \theta_\varepsilon = \theta_\sigma$

Material properties

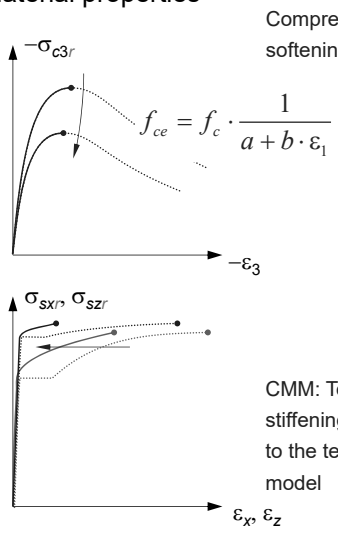

In the simplified Cracked Membrane Model, stress-free, rotating cracks that run perpendicular to the direction of the principal tensile strain are considered as in the classical compression field model. The crack direction θ_ρ is, therefore, a variable and not a given angle. The principal compressive direction of the concrete stresses at the cracks coincides with that of the principal strains.

For stress-free cracks - except for the index *r* - the same equilibrium conditions are obtained as for the classical compression field model (see figure). These relationships can be read directly from Mohr's circles.

The steel and bond stresses are treated according to the tension chord model according to slides 34-36.

Compression field models

Cracked membrane model with rotating cracks: Consideration of tension stiffening and compression softening

Equilibrium | Compatibility | Material properties

Consideration of tension stiffening via modified stress-strain relationship of the reinforcement (CMM, Kaufmann & Marti 1998):

→ Equilibrium formulated in stresses at crack "r", consistent with basic assumption

→ Direct information on maximum stresses at the crack, crack spacing etc.

→ Direct link to limit analysis

→ Good prediction of load-deformation behaviour

$\sigma_z = \sigma_{c3r} \sin^2 \theta_\sigma + \rho_z \sigma_{szr}$

$\tau_{xz} = -\sigma_{c3r} \sin \theta_\sigma \cos \theta_\sigma$

and opening at $\alpha_r = \pi/2$

$\rightarrow \theta_\varepsilon = \theta_\sigma$

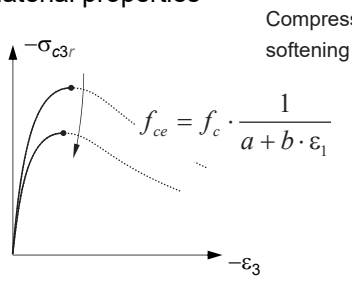

Compression softening

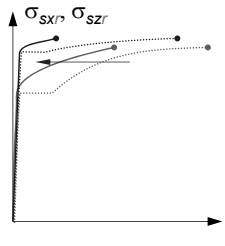

CMM: Tension stiffening according to the tension chord model

Compression field models

Cracked membrane model with rotating cracks: Consideration of tension stiffening and compression softening

Equilibrium | Compatibility | Material properties

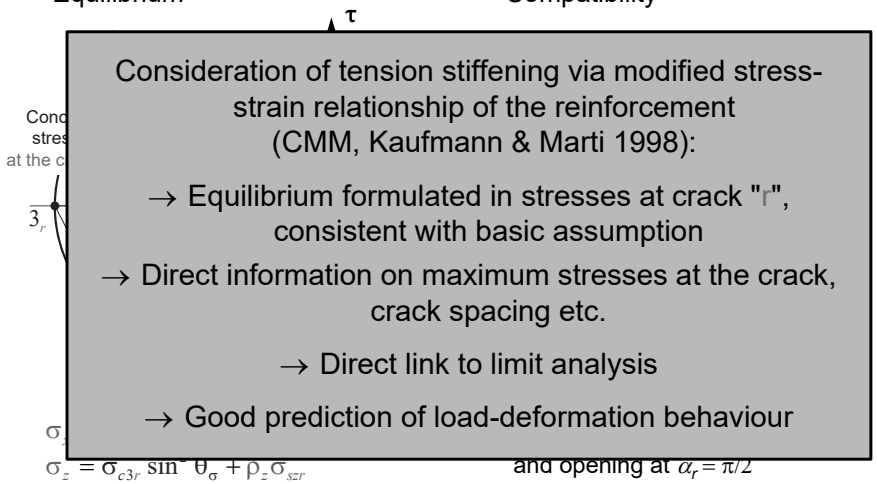

Consideration of tension stiffening via modified stress-strain relationship of the reinforcement (CMM, Kaufmann & Marti 1998):

→ Equilibrium formulated in stresses at crack "r", consistent with basic assumption

→ Direct information on maximum stresses at the crack, crack spacing etc.

→ Direct link to limit analysis

→ Good prediction of load-deformation behaviour

$\sigma_z = \sigma_{c3r} \sin^2 \theta_\sigma + \rho_z \sigma_{szr}$

$\tau_{xz} = -\sigma_{c3r} \sin \theta_\sigma \cos \theta_\sigma$

and opening at $\alpha_r = \pi/2$

$\rightarrow \theta_\varepsilon = \theta_\sigma$

Stress-strain relationship required for stresses at crack as a function of average strains

→ Tension chord model

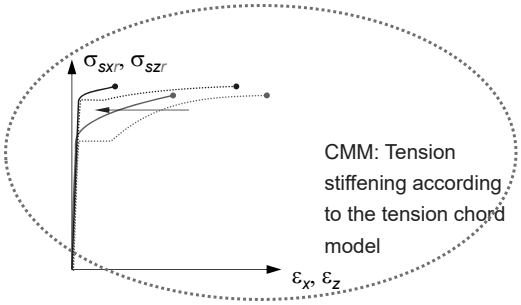

CMM: Tension stiffening according to the tension chord model

Compression field models

Cracked membrane model with rotating cracks: Consideration of tension stiffening and compression softening

Equilibrium

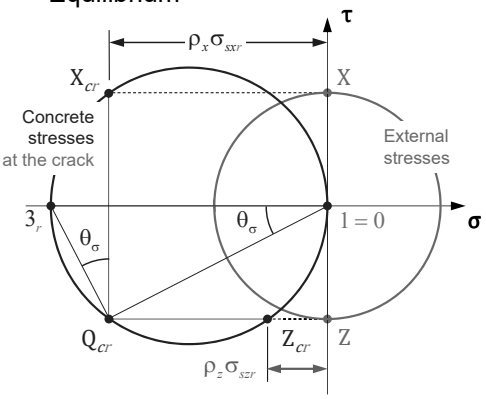

$$\sigma_x = \sigma_{c3r}\cos^2\theta_\sigma + \rho_x\sigma_{sxr}$$
$$\sigma_z = \sigma_{c3r}\sin^2\theta_\sigma + \rho_z\sigma_{szr}$$
$$\tau_{xz} = -\sigma_{c3r}\sin\theta_\sigma\cos\theta_\sigma$$

Compatibility

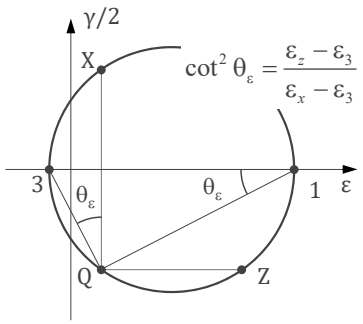

cracks parallel to θ_σ
and opening at $\alpha_r = \pi/2$
$\rightarrow \theta_\varepsilon = \theta_\sigma$

Material properties

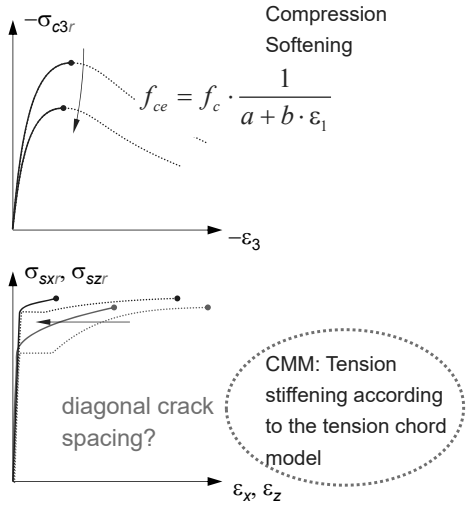

Compression field models

Cracked membrane model with rotating cracks: Determination of the maximum diagonal crack spacing

Exact solution

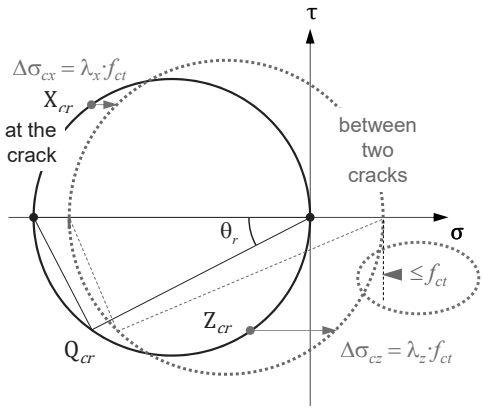

Maximum crack spacing for uniaxial tension in reinforcement direction: s_{rx0}, s_{rz0}
(according to the tension chord model)

$$s_{rx0} = \frac{f_{ct} \varnothing_x}{2\tau_{b0}} \frac{(1-\rho_x)}{\rho_x}$$

$$s_{rz0} = \frac{f_{ct} \varnothing_z}{2\tau_{b0}} \frac{(1-\rho_z)}{\rho_z}$$

Geometric relationship between s_{rx}, s_{rz} and diagonal crack spacing s_r

$$s_r = s_{rx} \sin\theta_r = s_{rz} \cos\theta_r$$

Parameters for crack distance $\lambda = 0.5...1$:
($\lambda = 1.0$: max. crack distance $s_r = s_{r0}$
$\lambda = 0.5$: min. crack distance $s_r = s_{r0}/2$)

$$\lambda = s_r / s_{r0}$$

$$\lambda_x = \frac{\Delta\sigma_{cx}}{f_{ct}} = \frac{s_{rx}}{s_{rx0}} = \frac{s_r}{s_{rx0} \sin\theta_r}$$

$$\lambda_z = \frac{\Delta\sigma_{cz}}{f_{ct}} = \frac{s_{rz}}{s_{rz0}} = \frac{s_r}{s_{rz0} \cos\theta_r}$$

Principal stress σ_{c1} between two cracks:

$$\sigma_{c1} = \frac{f_{ct}}{2}(\lambda_x + \lambda_z) - \frac{\tau_{xz}}{2}(\cot\theta_r + \tan\theta_r) + \sqrt{\left[\frac{\tau_{xz}}{2}(\cot\theta_r - \tan\theta_r) - \frac{f_{ct}}{2}(\lambda_x - \lambda_z)\right]^2 + \tau_{xz}^2} \leq f_{ct}$$

→ quadratic equation for maximum diagonal crack spacing s_{r0}

The crack distances in the reinforcement directions are geometrically linked to the diagonal crack distance (see figure on slide 30). The stresses in the concrete between the cracks result from the superposition of the diagonal compressive stress field acting at the crack faces (parallel to the cracks) with the tensile stresses, which are transferred to the concrete by the two reinforcements via the bond stresses.

The maximum diagonal crack spacing results from the condition that the principal stress in the centre between the cracks cannot exceed the tensile strength.

The parameter λ for the diagonal crack distance has the same meaning as for uniaxial loading in the tension chord model (theoretically $\lambda = 0.5 ... 1.0$).

Compression field models

Cracked membrane model with rotating cracks: Determination of the maximum diagonal crack spacing

Exact solution

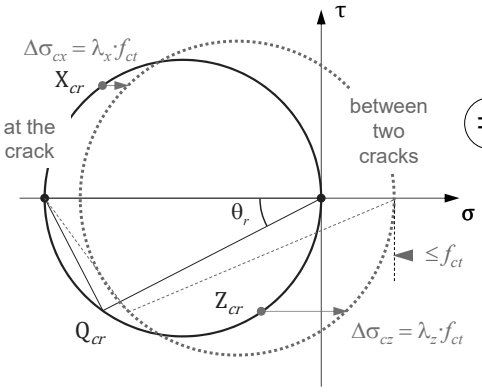

Approximation (symmetric / antisymmetric part of the composite)

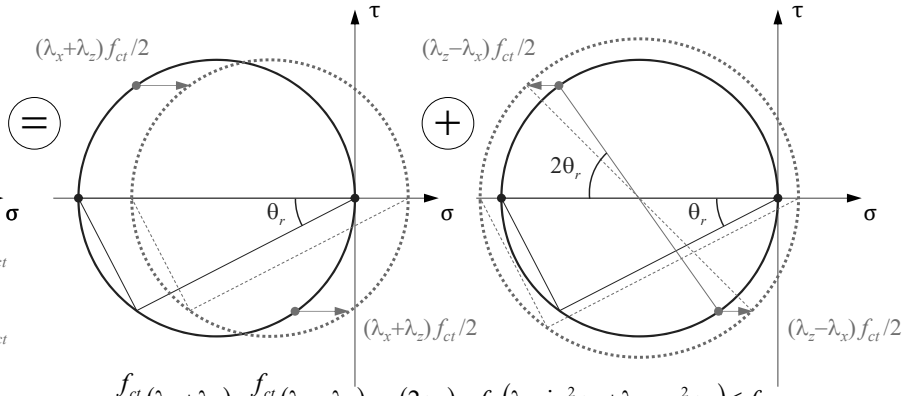

$$\sigma_{c1} \approx \frac{f_{ct}}{2}(\lambda_x+\lambda_z) - \frac{f_{ct}}{2}(\lambda_x-\lambda_z)\cos(2\alpha_r) = f_{ct}\left(\lambda_x \sin^2\alpha_r + \lambda_z \cos^2\alpha_r\right) \leq f_{ct}$$

Closed form approximate solution for maximum diagonal crack distance s_{r0}:

$$s_{r0} \approx \frac{1}{\frac{\sin\theta_r}{s_{rx0}} + \frac{\cos\theta_r}{s_{rz0}}}$$

The relationship for the maximum crack spacing can be simplified by breaking down the tensile stresses, which are transferred to the concrete by the two reinforcements via bond stresses. They are separated into a symmetric and an antisymmetric component. The principal tensile stress is approximated by neglecting the change in the principal direction between the cracks.

The resulting relationship for the maximum crack distance is sufficient in most cases (and an upper limit for the more accurate value) and is also used in standards today. It was derived earlier by Vecchio and Collins on the basis of plausibility considerations.

Compression field models

Cracked membrane model with rotating cracks: Determination of the maximum diagonal crack spacing

exact solution (function of τ_{xz}/f_{ct})

approximation $s_{r0} = \dfrac{1}{\dfrac{\sin\theta_r}{s_{rx0}} + \dfrac{\cos\theta_r}{s_{rz0}}}$

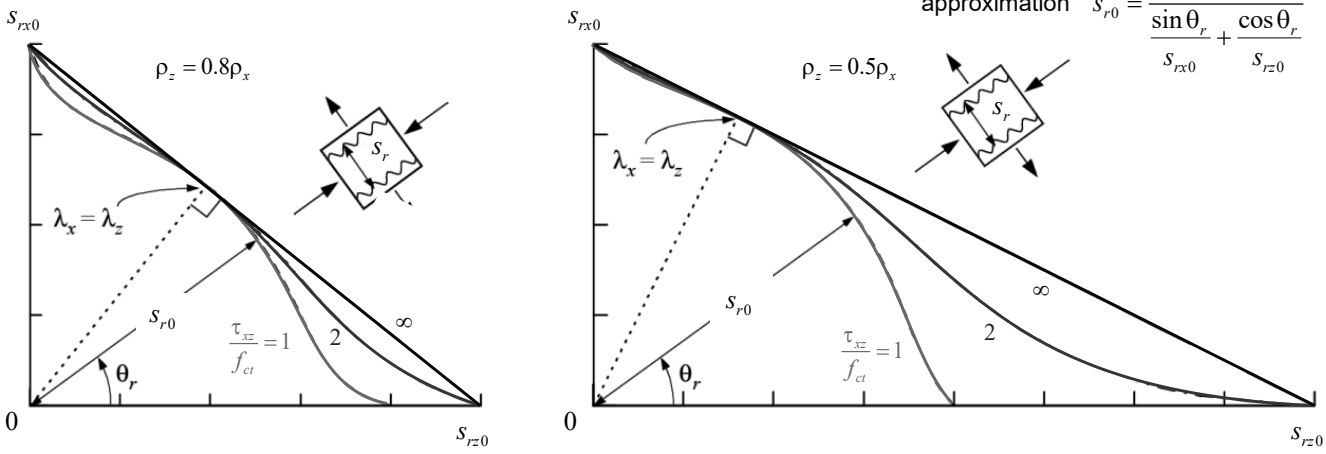

Membrane elements - Load-deformation behaviour

Reinforced concrete membrane element under monotonous load increase

1. Uncracked behaviour: Like homogeneous concrete membrane element (slight differences due to restraint shrinkage etc.)
2. Initial cracking approximately perpendicular to the principal tensile stress direction
3. Crack formation → Redistribution of internal forces → Change of principal stress directions immediately after crack formation
4. Cracked-elastic behaviour: Principal stress directions ± constant as long as both reinforcements remain elastic
5. Yielding of a reinforcemen
   → Decrease in stiffness –
   → New cracks (closer to t
6. Failure due to failure of th
   reinforcement (possibly re
   fails)

irrelevant for serviceability limit state

ıent of internal forces
ɔn-yielding reinforcement)
g of the other
s or aggregate interlock

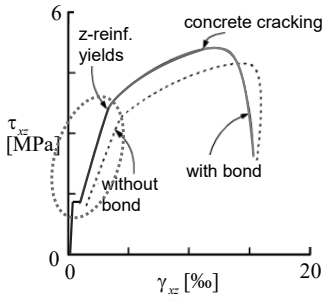

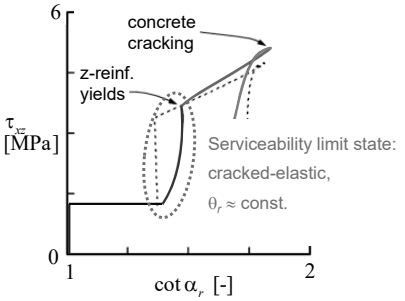

Repetition of the slide (4) shown in the introduction.

Compression field models

Cracked membrane model with rotating cracks

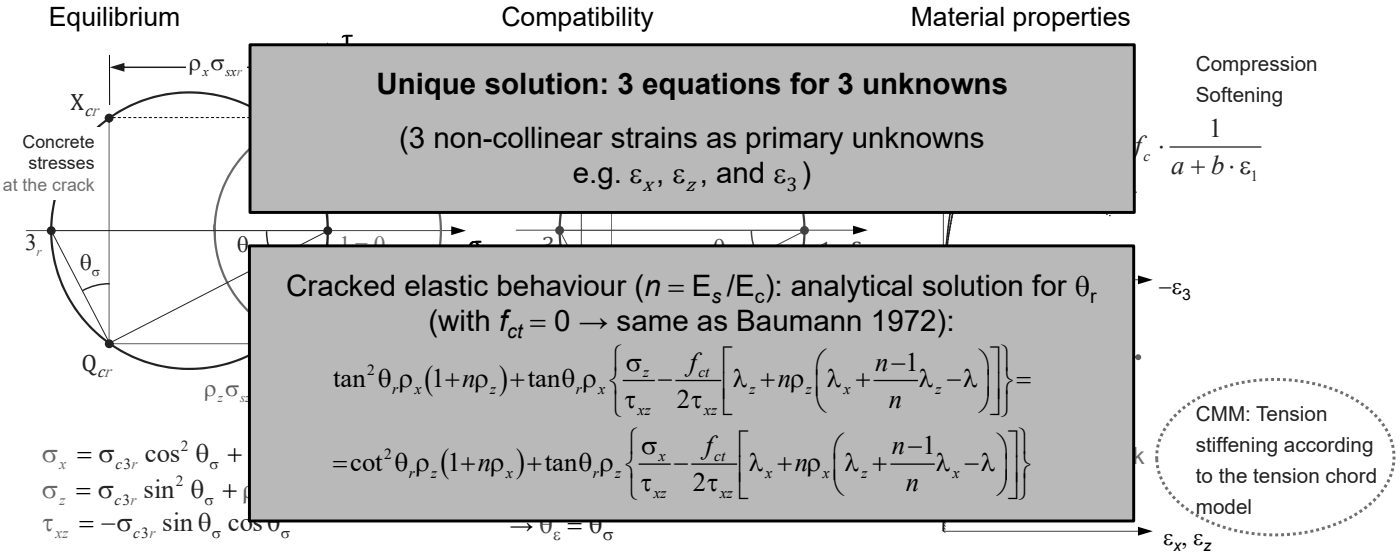

Here it is assumed that the stresses and strains in the quarter points between the cracks are characteristic of the behaviour of the element. With this assumption, an analytical approximate solution for the load-deformation behaviour can be derived (exact derivation in [4], p. 192).

For linear elastic material behaviour, the strains ε_x, ε_z, and ε_3 can be determined in the quarter points between the cracks via the stress in the concrete and in the reinforcement. If these are placed in the compatibility condition $\cot^2\theta_r = (\varepsilon_z - \varepsilon_3)/(\varepsilon_x - \varepsilon_3)$, the relationship for the crack inclination θ_r according to the slide is obtained.

The values of λ_x and λ_z are dependent on θ_r, so the solution requires an iterative numerical approach (but simple, only one equation with θ_r as it is the only unknown).

Additional remark

- If $\lambda = 0$ is used, the *Cracked Membrane Model* corresponds to the classic compression field model. This is therefore included as a special case in the general model.

Compression field models

Cracked membrane model with rotating cracks

Equilibrium | Compatibility | Material properties

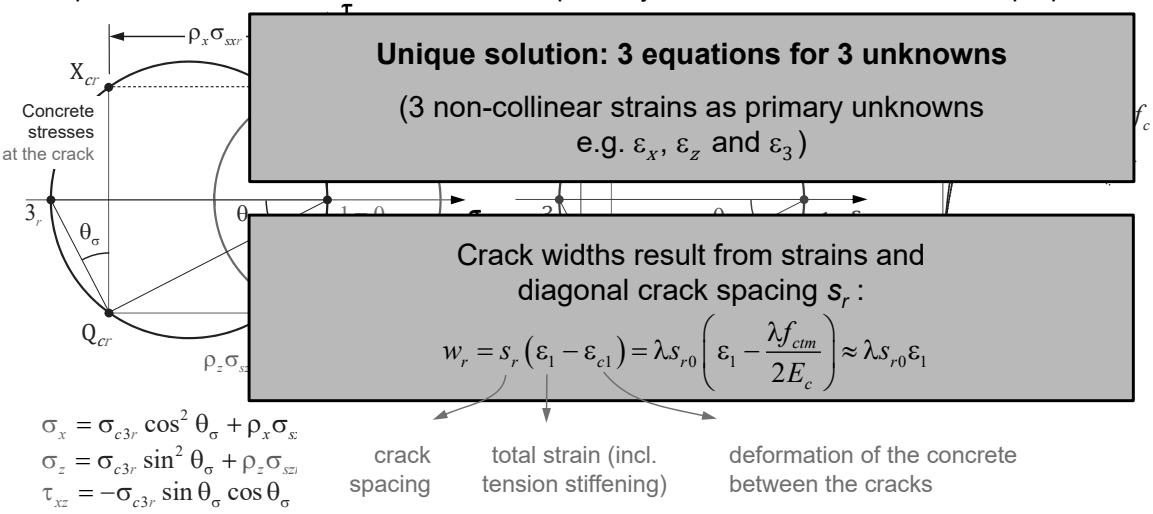

Unique solution: 3 equations for 3 unknowns

(3 non-collinear strains as primary unknowns
e.g. ε_x, ε_z and ε_3)

Crack widths result from strains and diagonal crack spacing s_r :

$$w_r = s_r\left(\varepsilon_1 - \varepsilon_{c1}\right) = \lambda s_{r0}\left(\varepsilon_1 - \frac{\lambda f_{ctm}}{2E_c}\right) \approx \lambda s_{r0}\varepsilon_1$$

Compression Softening

$$f_c \cdot \frac{1}{a + b\cdot\varepsilon_1}$$

$$\sigma_x = \sigma_{c3r}\cos^2\theta_\sigma + \rho_x\sigma_{sx}$$
$$\sigma_z = \sigma_{c3r}\sin^2\theta_\sigma + \rho_z\sigma_{szr}$$
$$\tau_{xz} = -\sigma_{c3r}\sin\theta_\sigma\cos\theta_\sigma$$

crack spacing | total strain (incl. tension stiffening) | deformation of the concrete between the cracks

CMM: Tension stiffening according to the tension chord model

Compression field models

Cracked membrane model with rotating cracks: strains in cracked membrane elements

Total strains $\{\varepsilon\}$ = strains in concrete between cracks $\{\varepsilon\}^{(c)}$ + strains due to crack kinematics $\{\varepsilon\}^{(r)}$

Contribution to total strain:

- $\{\varepsilon\}^{(c)}$ (average c
- $\{\varepsilon\}^{(r)}$ (smeared c

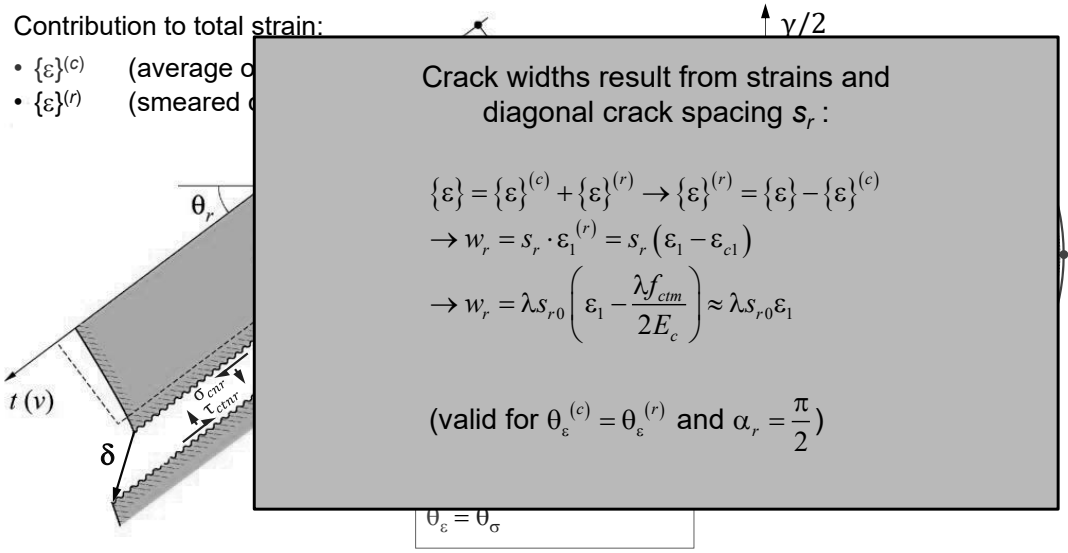

Crack widths result from strains and diagonal crack spacing s_r :

$$\{\varepsilon\} = \{\varepsilon\}^{(c)} + \{\varepsilon\}^{(r)} \rightarrow \{\varepsilon\}^{(r)} = \{\varepsilon\} - \{\varepsilon\}^{(c)}$$

$$\rightarrow w_r = s_r \cdot \varepsilon_1^{(r)} = s_r \left(\varepsilon_1 - \varepsilon_{c1}\right)$$

$$\rightarrow w_r = \lambda s_{r0} \left(\varepsilon_1 - \frac{\lambda f_{ctm}}{2E_c}\right) \approx \lambda s_{r0} \varepsilon_1$$

(valid for $\theta_\varepsilon^{(c)} = \theta_\varepsilon^{(r)}$ and $\alpha_r = \frac{\pi}{2}$)

$\theta_\varepsilon = \theta_\sigma$

Total strains $\{\varepsilon\}$:

$\{\varepsilon\} = \{\varepsilon\}^{(c)} + \{\varepsilon\}^{(r)}$

$\theta_\varepsilon \neq \theta_\varepsilon^{(c)} \neq \theta_\varepsilon^{(r)}$

$\theta_\varepsilon^{(c)} = \theta_\varepsilon^{(r)}$ if $\theta_r = \theta_\sigma$ and $\alpha_r = \pi/2$ (local variation neglected)

The total strains of a reinforced concrete membrane element can be interpreted as the sum of the average crack-related strains and average strains of the concrete between the cracks, as shown in the introduction. The crack width then results as the product of the average principal crack-related strain $\varepsilon_1^{(r)}$ with the diagonal crack spacing s_{rm}.

In the Cracked Membrane Model only total strains have been considered so far. The average principal strain due to cracking $\varepsilon_1^{(r)}$ can be calculated, by deducting the average principal strain of the concrete between the cracks, $\varepsilon_1^{(c)}$from the total principal strain ε_1. The strains of the concrete between the cracks can basically be calculated from the stresses in the concrete between the cracks. It turns out, however that $\varepsilon_1^{(c)}$ in comparison with ε_1 can be neglected (for not very high reinforcement ratios), especially since only upper and lower limits can be specified for the diagonal crack distance s_{rm}.

Additional remark: Note that neglecting $\varepsilon_1^{(c)}$ does not mean that tension stiffening is neglected: The major influence of tension stiffening is captured by the lower value of ε_1 obtained due to the consideration of stress-strain relationships of the reinforcement expressing steel stresses at cracks as a function of average strains (TCM).

Compression field models

Cracked membrane model with rotating cracks

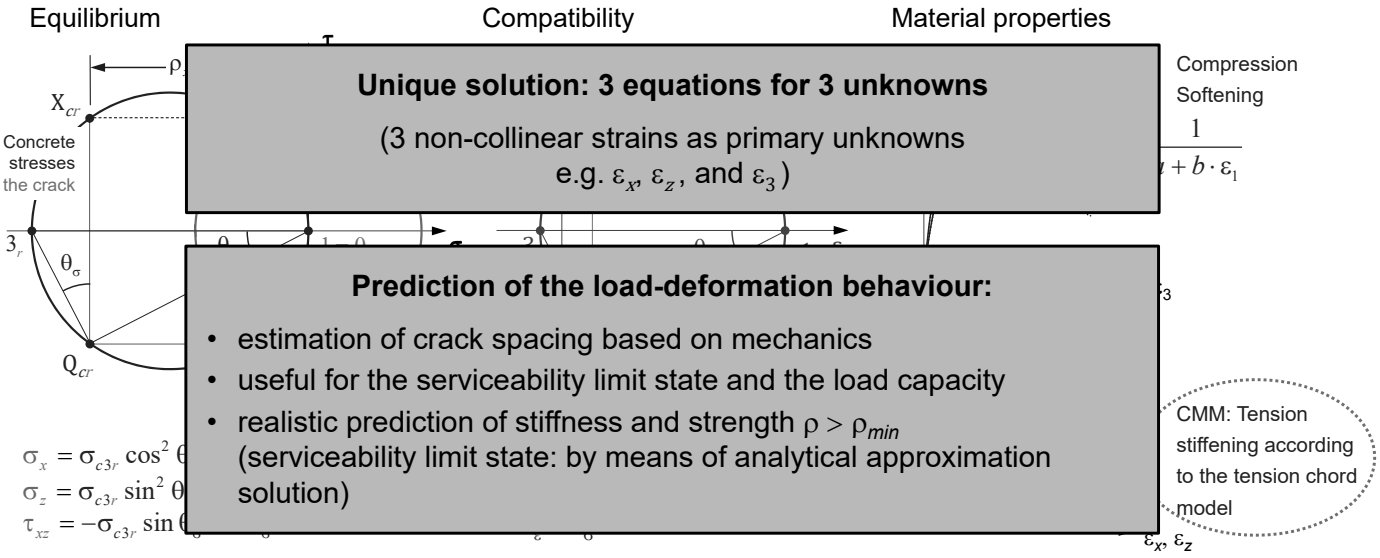

Unique solution: 3 equations for 3 unknowns

(3 non-collinear strains as primary unknowns
e.g. ε_x, ε_z, and ε_3)

Prediction of the load-deformation behaviour:

- estimation of crack spacing based on mechanics
- useful for the serviceability limit state and the load capacity
- realistic prediction of stiffness and strength $\rho > \rho_{min}$
  (serviceability limit state: by means of analytical approximation solution)

Compression field models

Cracked membrane model with rotating cracks: Comparison with experiment: load-deformation behaviour

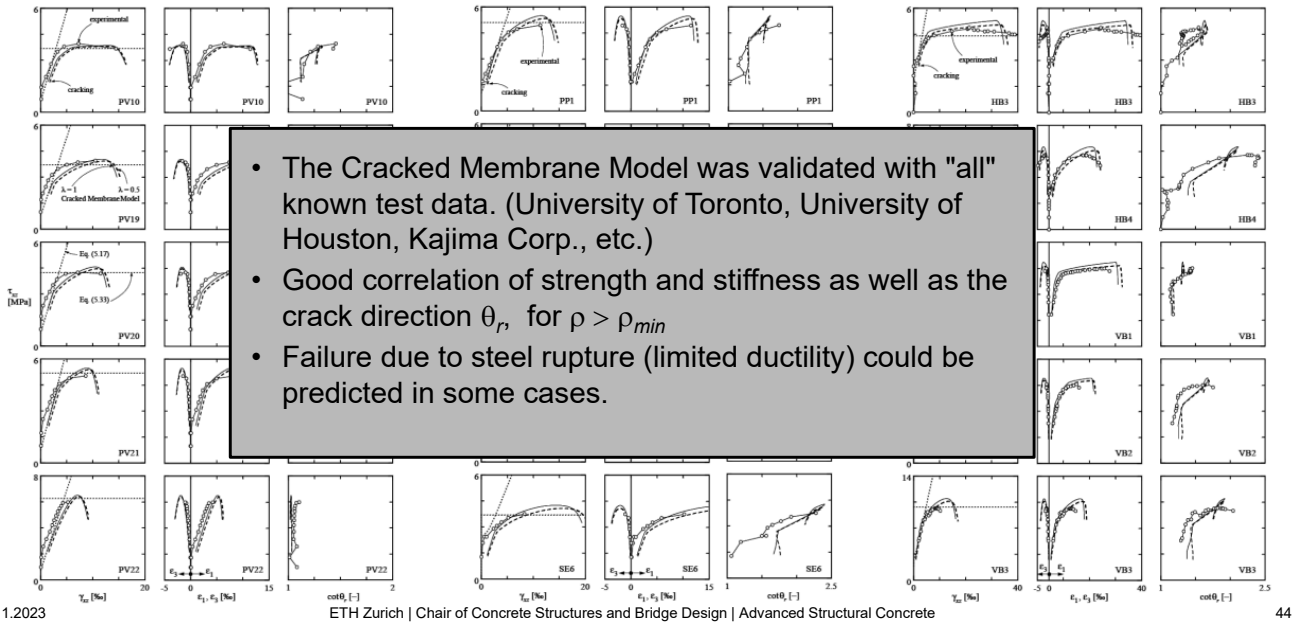

- The Cracked Membrane Model was validated with "all" known test data. (University of Toronto, University of Houston, Kajima Corp., etc.)
- Good correlation of strength and stiffness as well as the crack direction θ_r, for $\rho > \rho_{min}$
- Failure due to steel rupture (limited ductility) could be predicted in some cases.

Additional remark

For small loads, the Cracked Membrane Model overestimates the tension stiffening; the general equation for crack spacing applies only to a limited extent.

- As with tension elements, the minimum and maximum diagonal crack spacing s_r differ by a factor of 2 ($\lambda = 0.5... 1$). For the crack distances s_{rx} and s_{rz} in the reinforcement directions, however, this relationship obviously no longer applies, since they are geometrically linked with $s_r = \lambda s_{r0}$. (see earlier slides, $s_{rx} = s_r / \sin\theta_r$, $s_{rz} = s_r / \cos\theta_r$).

- Due to the prevailing uncertainty regarding s_r, the closed analytical approximation formula is usually sufficient for practical applications.

Compression field models

Cracked membrane model with rotating cracks: Comparison with experiments: crack widths

Tests by Proestos (2014): membrane elements 1525-1525-355 mm under uniform load

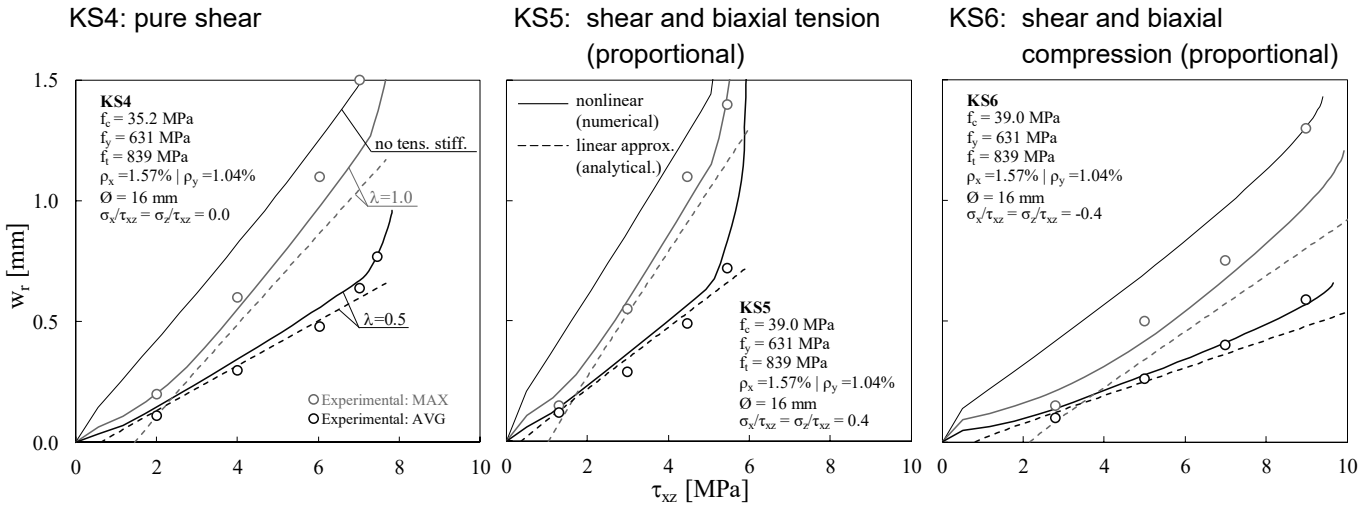

To date, only a few test results are available which are suitable for a comparison of the measured and calculated crack widths. The main reason for this is that the crack widths (distances, opening/width, slip) were only systematically measured in few individual test series. There is therefore only limited information on the crack kinematics and in particular practically no data on the crack slip (parallel crack face displacements).

The measurement of crack kinematics is more difficult than it seems at first glance. The cracks are not straight even under uniform loading, and the crack spacing varies greatly. Crack opening and slip are not constant even for a single crack, but vary along its length. The crack width measurement "by hand" (crack magnifier, crack scale, ...) is often implicitly carried out at the point where the crack (initially) is the widest. These crack widths are then averaged over several cracks and specified as "mean" crack widths. An averaging of the crack widths along the crack is hardly feasible when measuring "by hand". Crack slip can hardly be detected with conventional measuring methods (if the location of the crack is not known beforehand so that a sensor could be mounted).

Better experimental data can be obtained by evaluating measurements with digital image correlation. In the current experiments at ETH Zurich, such measurements are carried out, and the crack kinematics are determined semi-automatically ("automated crack detection and measurement“, ACDM).

The slide shows predictions according to CMM and results of the Proestos experiments (2014). The comparison shows an excellent correlation with the measured crack widths. It can be seen that even the analytical approximate solution for the serviceability limit state provides sufficiently accurate results (crack slip was not measured in these tests either so that no validation is possible in this respect). The slight underestimation of w_{rmax} may be due to the fact that the maximum crack widths per crack were measured.

Compression field models

Cracked membrane model with rotating cracks: Application limits / open questions

Fictitious, rotating, stress-free cracks vs real, interlocking cracks

- Unsatisfactory prediction for $\rho < \rho_{min}$, no convergence for uniaxial reinforcement

→ General cracked membrane model considers fixed, interlocking cracks

→ Most general solution for:

  - Only one group of parallel cracks with equal distances over the entire element
  - Reinforcement is considered as equivalent stress (constant over rebar spacing and membrane element thickness).

So far, the simplified CMM has been treated with stress-free cracks.

In its general formulation, the Cracked Membrane Model takes into account general cracks that are neither stress-free nor coincide with the principal strain directions.

Following, this general model is explained in principle without going into the details.

Compression field models

Cracked membrane model with fixed cracks: General solution, with aggregate interlock

Membrane element

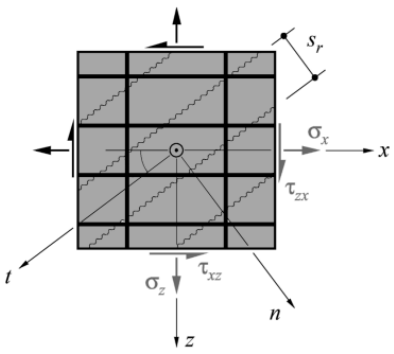

Stresses at crack / equilibrium

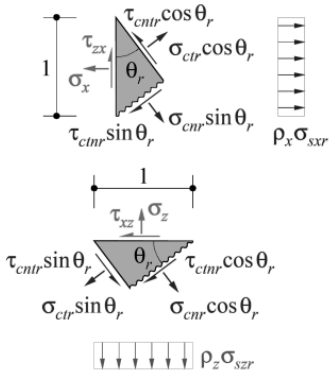

Displacements & strains

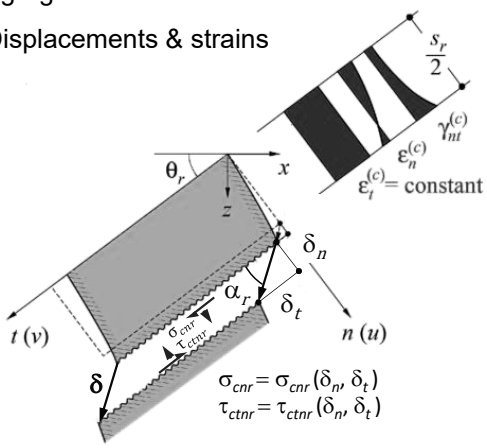

Required material properties:

- Constitutive relationships of concrete and reinforcement
- Bond-slip relationship

$$\sigma_x = \rho_x\sigma_{sxr} + \sigma_{cnr}\sin^2\theta_r + \sigma_{ctr}\cos^2\theta_r - \tau_{ctnr}\sin(2\theta_r)$$

$$\sigma_z = \rho_z\sigma_{szr} + \sigma_{cnr}\cos^2\theta_r + \sigma_{ctr}\sin^2\theta_r + \tau_{ctnr}\sin(2\theta_r)$$

$$\tau_{xz} = (\sigma_{cnr} - \sigma_{ctr})\sin\theta_r\cos\theta_r - \tau_{ctnr}\cos(2\theta_r)$$

$\varepsilon_n^{(c)}$, $\varepsilon_t^{(c)}$, $\gamma_{nt}^{(c)}$ are independent of the coordinate t; thus $\partial\gamma_{nt}^{(c)}/\partial t = 0$, i.e. $\partial\varepsilon_t^{(c)}/\partial n = 0$ and $\varepsilon_t^{(c)}$ = constant

($\varepsilon_n = \partial u/\partial n$, $\varepsilon_t = \partial v/\partial t$, $\gamma_{nt} = \partial u/\partial t + \partial v/\partial n$)

The slide shows the basic assumptions and designations of the general cracked membrane model.

Compression field models

Cracked membrane model with fixed cracks: General solution, with aggregate interlock

Membrane element

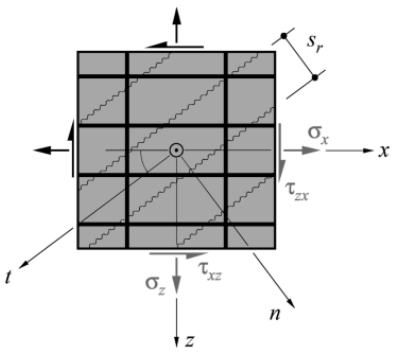

Required material properties:

- Constitutive relationships of concrete and reinforcement
- Bond-slip relationship

General solution method (for given crack inclination and spacing)

Assumption / estimation of 7 primary unknowns:

- 3 stress components at crack σ_{sxr}, σ_{szr}, σ_{ctr}
- 2 crack displacements (opening and slip) δ_n, δ_t
- 2 concrete displacements at the crack u_{cr}, v_{cr}

Determine the concrete stresses at the crack σ_{cnr}, τ_{ctnr} via the crack opening and slip δ_n, δ_t using the aggregate interlock relationship $\sigma_{cnr} = \sigma_{cnr}(\delta_n, \delta_t)$, $\tau_{ctnr} = \tau_{ctnr}(\delta_n, \delta_t)$.

The bond stress as well as the stresses, strains, and displacements in the concrete and reinforcement are determined by means of the differential equilibrium and the compatibility conditions. This is done starting from the crack ($n = s_r/2$), in infinitesimal steps dn going towards $n = 0$.

Iteration until the following conditions are met (7 equations for 7 unknowns):

- 3 equilibrium conditions at the crack
- 2 components of the concrete displacements u_c, v_c and 2 reinforcement displacements u_{sx}, u_{sz} must vanish in the middle between two cracks.

In the general case the consideration of a set of parallel cracks leads to a system of 7 equations with 7 unknowns.

Compression field models

Cracked membrane model with fixed cracks: Application limits / open questions

Lack of experimental data (measured directly, not biased by the measurement)

- Stresses in concrete cannot be measured experimentally (they are usually estimated by surface strains).
- Local measurements of the stresses in the steel with conventional instrumentation (e.g. with strain gauges, ...) depend on the location of the measurement (near or far from the crack). In addition, they usually disturb the bond.

→ The most commonly used relationships for tension stiffening and compression softening have been insufficiently validated with experiments.

→ Today, it is possible to measure the steel strains continuously along an embedded reinforcing bar using fibre optic strain sensing without disturbing bond; new insights from experimental testing of panels

- Crack kinematics (in particular the crack slip) are difficult to record with conventional instrumentation (unless the location of the cracks is known in advance); only limited experimental data are available.
- Push-off tests are not necessarily representative of aggregate interlock in biaxially reinforced elements.

→ Aggregate interlock relationship still needs to be validated.

→ Today, with 3D Digital Image Correlation (DIC) and Automatic Crack Detection & Measurement of their kinematics (ACDM) new insights into the behaviour are gained

At ETH Zurich, experiments are currently being carried out in LUSET to help clarify these points.

Measured or calculated?

Determination of stress and strain state in experiments

Equilibrium

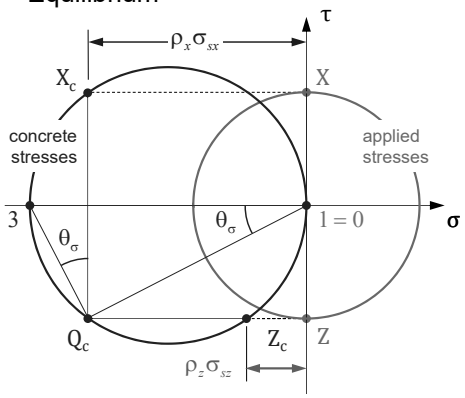

$$\sigma_x = \sigma_{c3}\cos^2\theta_\sigma + \rho_x\sigma_{sx}$$
$$\sigma_z = \sigma_{c3}\sin^2\theta_\sigma + \rho_z\sigma_{sz}$$
$$\tau_{xz} = -\sigma_{c3}\sin\theta_\sigma\cos\theta_\sigma$$

Compatibility

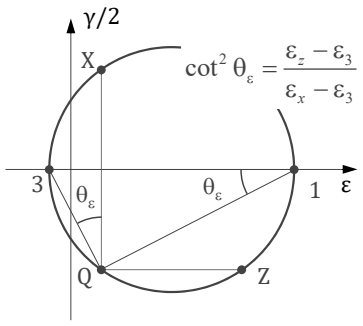

cracks parallel to θ_σ
and opening at $\alpha_r = \pi/2$
$\rightarrow \theta_\varepsilon = \theta_\sigma$

Material properties

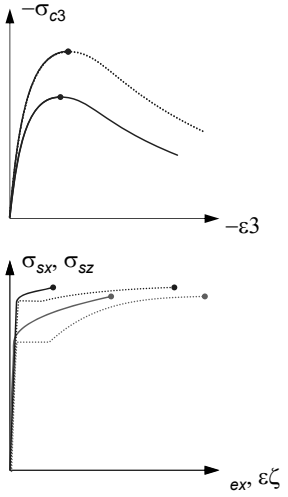

With conventional measuring methods the average strains and the applied loads can be measured. This was done in previous tests on membrane elements.

These measurements were then used to calculate the stresses in concrete and reinforcement, assuming a characteristic curve of the reinforcement and the concrete: In the MCFT by assuming "average" steel stresses = characteristic curve of the bare reinforcement, in the CMM under prerequisite of the tension chord model per reinforcement direction. When many MCFT publications talk about "measured stresses" in the reinforcement (and sometimes also in the concrete), this is therefore misleading: The stresses were not measured, but are obtained by assuming a material law that cannot be determined directly from a material test.

With continuous strain measurements along the entire length of the reinforcing bar, however, the stresses in the reinforcement can actually be determined directly from the well known characteristic curve of the bare steel. However, this must not affect the bond. Today, this is done at ETH Zurich with fiber-optic strain measurements.

Thus, it is no longer necessary to postulate material laws for reinforcement and concrete (taking compression softening and tension stiffening into account), but rather, these result from the measured stresses - with which the assumptions can be validated.

If, in addition, the strains of the surface are recorded over the entire surface and the crack kinematics are determined from this (see slide 53), then aggregate interlock relationships (crack opening and slip <-> normal and shear stress at the crack) can be determined.

Measured or calculated?

Determination of stress and strain state in experiments with conventional measurements

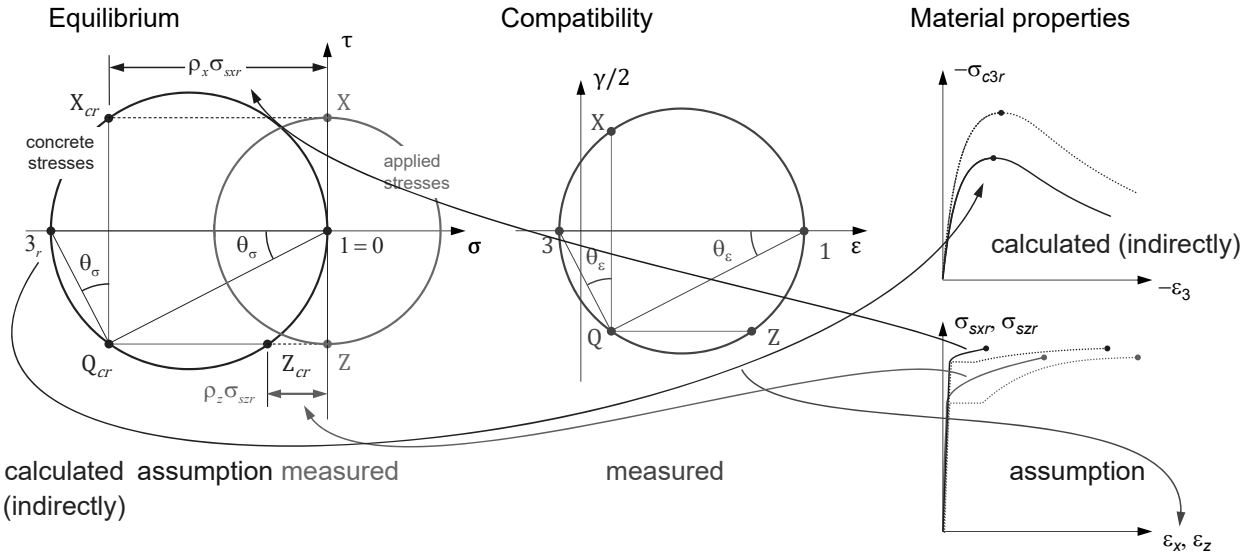

Measured or calculated?

Determination of stress and strain state in experiments with continuous strain measurement (fibres)

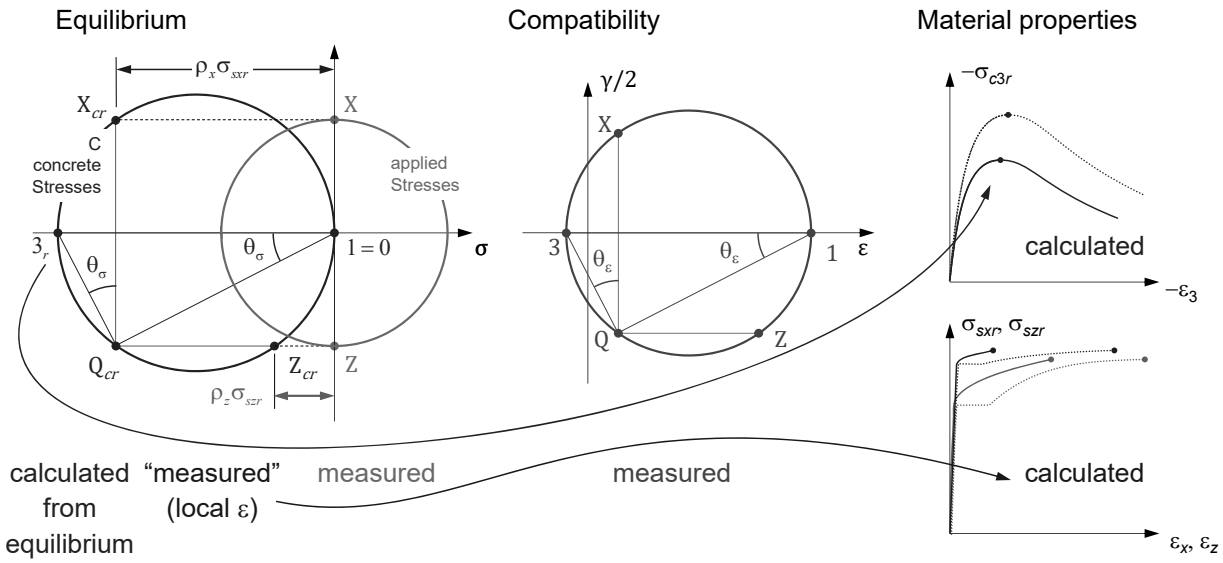

Compatibility and deformation capacity of membrane elements: Summary

Summary

- The Cracked Membrane Model (general formulation with aggregate interlock) requires (numerical) solving of seven highly nonlinear equations with seven unknown quantities: very complex
- Simplification with Cracked Membrane Model (without aggregate interlock) = combination of the classic compression field models with the tension chord model:
  - Stress-free cracks parallel to the direction of the principal strains (variable crack direction, fictitious cracks)
  - Tension stiffening effect of the concrete between the cracks according to the tension chord model (without influence on resistance of reinforcement, indirect influence on ultimate load as strains become smaller → higher concrete compressive strength)
  - Concrete compressive strength as a function of strain state (transverse strain)

- The Cracked Membrane Model (without aggregate interlock) generally provides good agreement with test results. In the serviceability limit state (elastic reinforcement), the analytical approximation solution can be easily applied.
- The consideration of the aggregate interlock (general formulation of the Cracked Membrane Model) would make sense if the element is only reinforced in one direction or if the reinforcement ratio is very low in the other direction.

Annex

Shear Panel Tester, University of Toronto (1979)

In-plane loading (3 stress resultants)

Applied in-plane loads
perpendicular and parallel to element edge

→ principal direction of applied loads variable

→ reinforcing bars parallel to element edges

Element size 890-890-70 mm

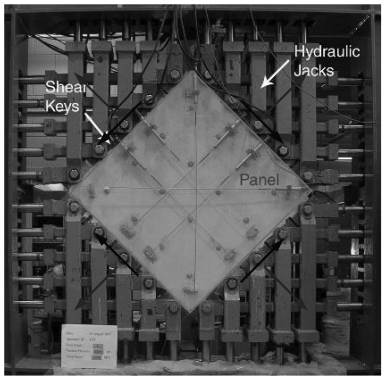

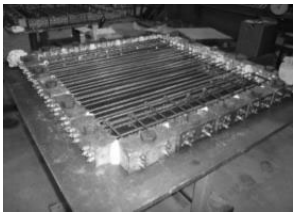

In the *Shear Panel Tester,* elements with dimensions of 890x890x70 mm can be tested under pure membrane loading (3 stress resultants: membrane (in-plane) forces $\{n_x, n_z, n_{xz}\}$), with any principal direction of the applied stress.

The load is applied by 40 hydraulic actuators parallel to the element plane (resp. 37 hydraulic actuators and 3 pendulum rods). The load is introduced via five load introduction elements on each side of the element. At each load introduction element, two hydraulic actuators act in the element plane at an angle of +45° or -45° to the element edge (transmitted via a sophisticated scissor system). By varying the hydraulic actuator forces, the desired membrane load (n_n and n_{tn}) can be set (equal hydraulic actuator forces with same sign = compression or tension n_n, equal hydraulic actuator forces with opposite sign = shear n_{tn} , etc.). The reinforcement runs through holes in the load introduction elements and is bolted to these on their rear side.

Since the principal direction of the applied membrane (in-plane) stresses is variable (shear and normal forces in the element plane in any combination), the elements can always be reinforced parallel to the element edges.

Due to the limited dimensions, very thin reinforcing bars and a concrete with a reduced maximum aggregate size are used, which must be taken into account when interpreting the test results.

Shell Element Tester, University of Toronto (1984 / 2009)

General loading (8 stress resultants)

Applied loads in-plane and out-of-plane, perpendicular to element edge

→ principal direction of applied loads constant

→ reinforcing bars at angle to element edges

Element size 1,524-1,524-350 mm

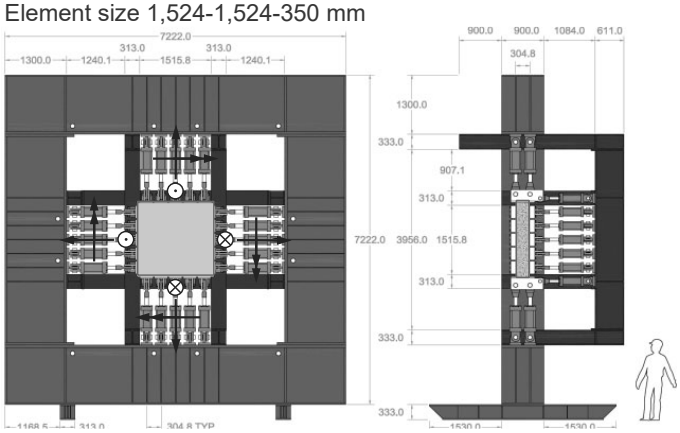

In the *Shell Element Tester,* elements with dimensions of 1,524x1,524x400 mm can be tested under general shell loading (8 stress resultants): membrane (in-plane) forces { n_x, n_z, n_{xz} }, bending and twisting moments { m_x, m_z, m_{xz} }, and transverse (out-of-plane) shear forces { v_x, v_z }), with constant principal direction of the applied membrane load.

The load is applied via 60 servo-hydraulically controlled actuators (40 acting in the plane of the element, capacity 1 MN each and 20 acting out of the plane of the element, capacity 0.5 MN each, 60 control circuits). The load is applied via five yokes on each side of the element. Each yoke is equipped with three actuators: two actuators parallel to the element plane and perpendicular to the element edge, and one actuator perpendicular to the element plane. While the latter corresponds to the applied transverse shear force v_n, the desired combination of membrane and bending stress (n_n and m_n) can be set by varying the two actuator forces parallel to the element plane (equal actuator forces with the same sign = pure compression or tension n_n, equal actuator forces with opposite sign = pure bending m_n, etc.). Twisting moments m_{tn} can be applied by corner forces $\pm 2m_{tn}$ acting perpendicular to the element plane (see lecture on plates, equivalence of corner forces and twisting moments).

The principal direction of the applied membrane forces is constant in this test facility (parallel to the element edges). Tests with alternating principal stress direction of the load (for example first longitudinal compression, then shear) are therefore not possible. In order to investigate shear stress with respect to the reinforcement directions, the elements are reinforced at an angle to the element edges; the reinforcement is welded to blocks which are bolted to the yokes.

The dimensions of the elements allow for the use of standard reinforcement diameters and concrete with standard maximum aggregate size.

Large Universal Shell Element Tester LUSET, ETH Zurich (2017)

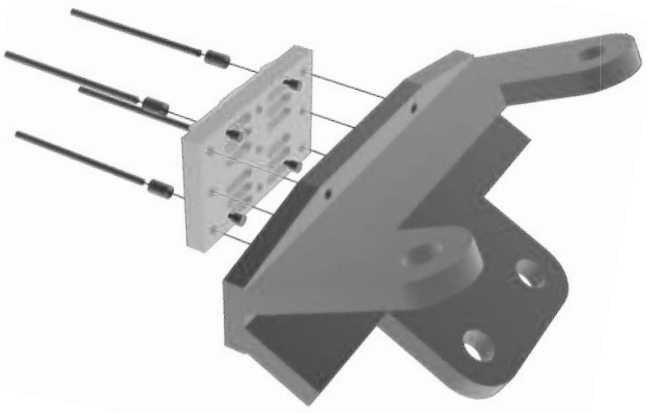

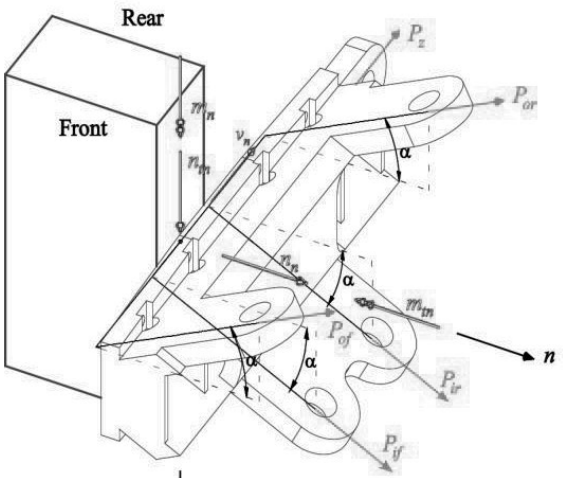

Load introduction

20 yokes, 20 blocks bolted to yokes

reinforcing bars with threaded ends and bar couplers (e.g. Bartec)

$$v_n = \frac{P_z}{0.4\,\mathrm{m}}$$

$$n_n = \frac{P_{of} + P_{if} + P_{or} + P_{ir}}{0.4\,\mathrm{m}} \cdot \cos\alpha$$

$$n_{tn} = \frac{-P_{of} + P_{if} - P_{or} + P_{ir}}{0.4\,\mathrm{m}} \cdot \sin\alpha$$

$$m_n = \frac{\left(P_{or} - P_{of}\right) \cdot 1.5e + \left(P_{ir} - P_{if}\right) \cdot 0.5e}{0.4\,\mathrm{m}} \cdot \cos\alpha$$

$$m_{tn} = \frac{-\left(P_{or} - P_{of}\right) \cdot 1.5e + \left(P_{ir} - P_{if}\right) \cdot 0.5e}{0.4\,\mathrm{m}} \cdot \sin\alpha$$

The load is applied by 100 servo-hydraulically controlled actuators (80 acting in the plane of the element, capacity each approx. 1.5 MN, and 20 acting out of the plane of the element, capacity each approx. 1.3 MN, 20 control circuits).

The load is transferred via five yokes on each side of the element. Each yoke has five actuators, see figure: two actuators parallel to the element plane at an angle of +26.56° (outside, inclination +1:2) or -26.56° (inside, inclination -1:2) and one actuator perpendicular to the element plane. The latter corresponds to the applied transverse (out-of-plane) shear force v_n. By varying the four actuator forces parallel to the element plane, the desired combination of membrane and bending stress (n_n, n_{tn} und m_n, m_{tn}) can be set, for example:

- Four equal actuator forces with the same sign = pure compression or tension n_n
- Four equal actuator forces, outside/inside opposite sign = pure membrane shear n_n
- Front two actuators tension, rear two actuators compression = bending moment m_n
- Actuators from front to rear alternating tension-compression = twisting moment m_{tn}

In the latter two cases, the forces of the inner and outer actuators must be inversely proportional to their lever arm in order to apply pure bending and twisting moments.

In summary, the five actuators per yoke can be used to apply the five stress resultants n_n, n_{tn} and m_n, m_{tn} and v_n in any magnitude. The sixth degree of freedom (rotation about the *z*-axis = perpendicular to the element plane, through which the axes of the 4 actuators lying parallel to the element plane run) is free. The corresponding rotations are only restrained by the element (specimen). In order to avoid the resulting disruptive influences of the dead weight of the lateral yokes and presses, their weight is compensated by gas tension springs anchored to the reaction frame (approximately constant forces at variable stroke).

Large Universal Shell Element Tester LUSET, ETH Zurich (2017)

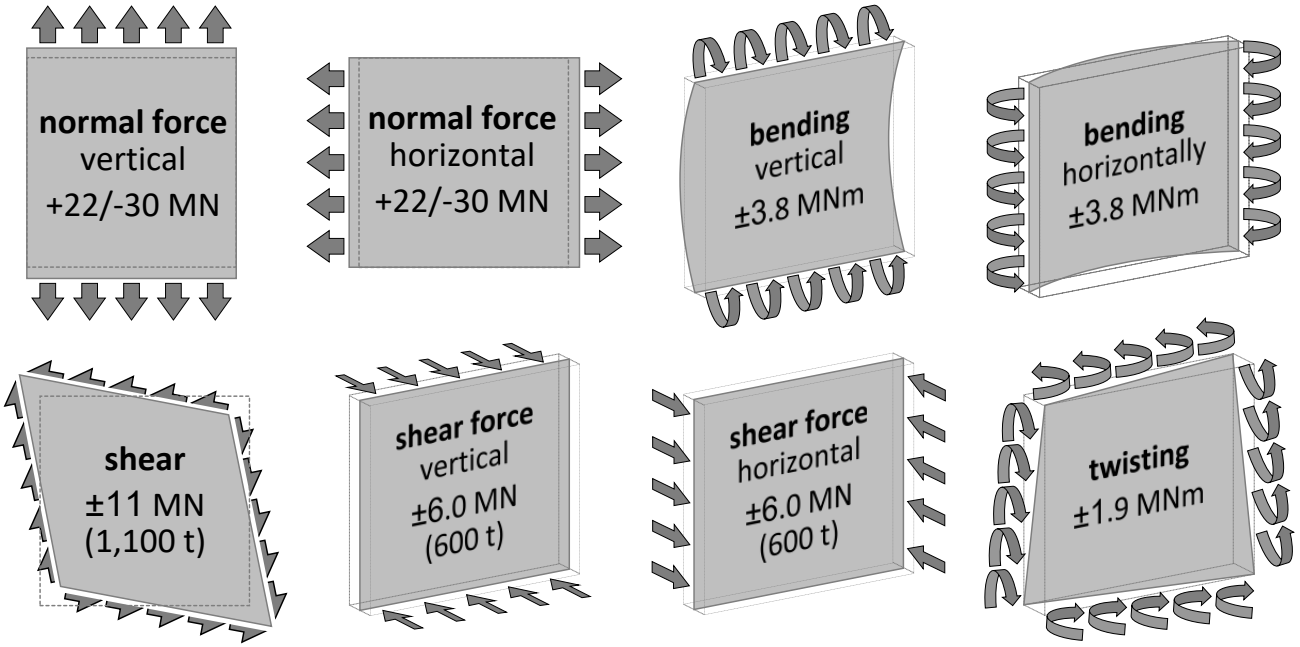

Large forces are required to test elements made of high-strength concrete.

SN: The 30 MN compression corresponds to the weight force of approx. 35 RE460 locomotives ("Lok 2000"), which stapled on each other would correspond to a tower higher than the Prime Tower in Zurich.

Large Universal Shell Element Tester LUSET, ETH Zurich (2017)

The reaction frame of LUSET is supported and partially located in the basement, for which an opening had to be cut into the floor slab of the lab.

The structural steelwork, the assembly of the reaction frame, and the hydraulic piping were completed in autumn of 2016. The assembly was essentially carried out in five parts (four parts of the frame in plane and one frame out of plane, each weighing approx. 20 t, corresponding to the combined capacity of the two 10 t-lab cranes).

Large Universal Shell Element Tester LUSET, ETH Zurich (2017)

The installation of the yokes was complex because they cannot be mounted individually (eyebar pieces are "nested"). The actuators could therefore only be mounted after the installation of the yokes (connected by means of a dummy element).

Large Universal Shell Element Tester LUSET, ETH Zurich (2017)

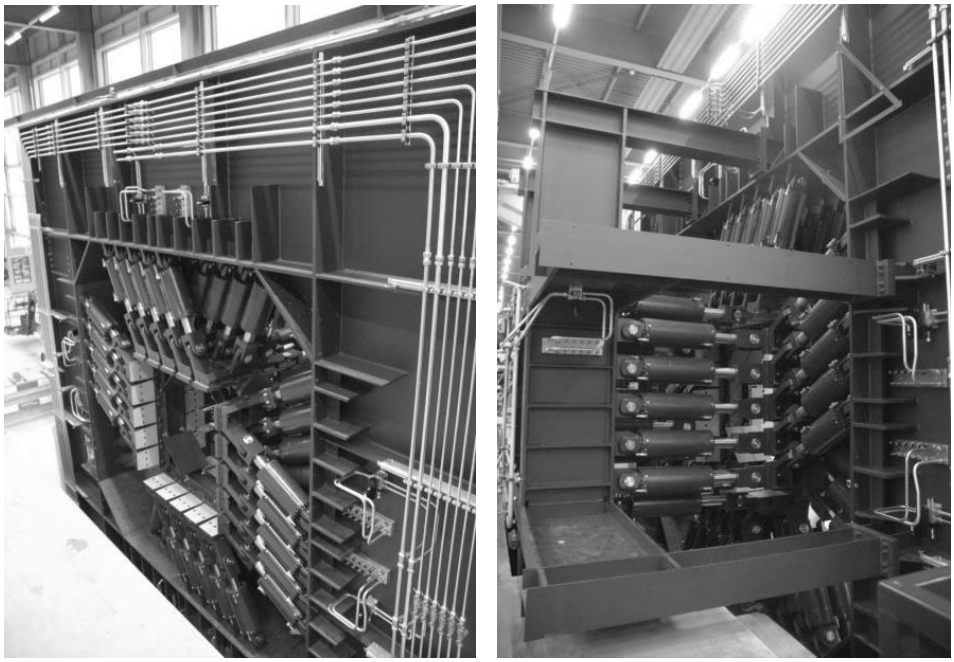

After the assembly of the frame and the lifting of the yokes, a total of 100 actuators (80 actuators in-plane, 20 actuators out-of-plane) were installed.

After installing the actuators and oil hydraulics, the measuring and control technology was wired (one internal displacement sensor and one load cell per actuator, one control valve with position monitoring and two pressure sensors per control circuit, one tilt sensor per yoke). Also the 20-channel control system was installed and specifically adapted to the requirements of LUSET. The scalable, digital control system (low-level real-time controller in C++, high level controller in MATLAB) has a very flexible design and can be adapted to a wide variety of configurations and test types, in load or displacement control.

Large Universal Shell Element Tester LUSET, ETH Zurich (2017)

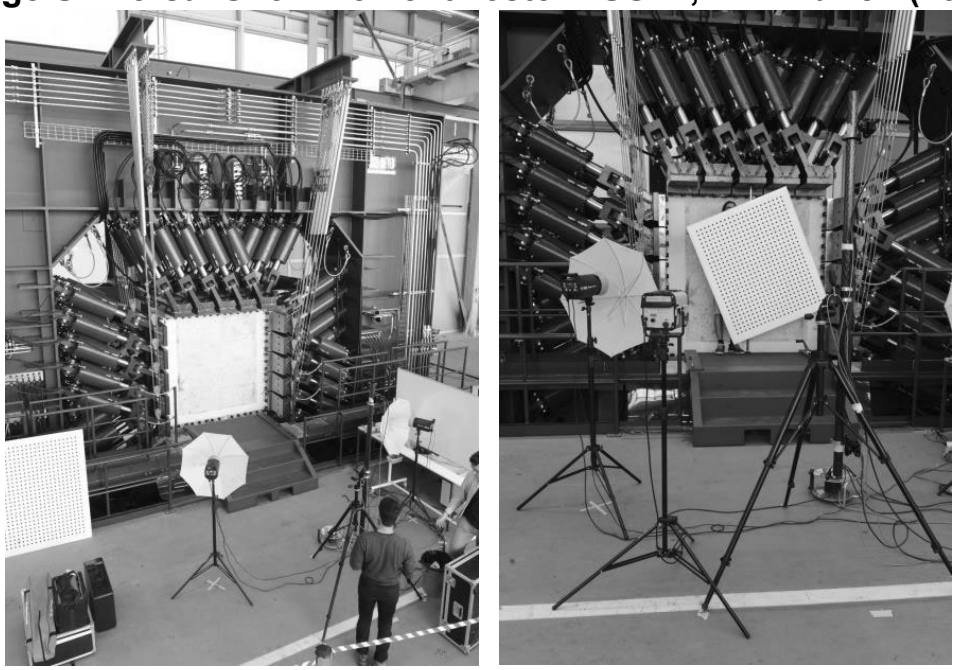

In addition to the force and displacement measurements of the actuators, the tests are instrumented with two different measuring systems.

Glass fibres are attached to the reinforcing bars of the elements, with which the strain of the steel can be measured continuously over the entire bar length via optical reflection (Rayleigh backscatter analysis). Due to the small dimensions of the fibres, the behaviour of the elements or the bond are not significantly biased.

The measuring technique is supplemented by digital image correlation systems, with which the entire surface is measured in 3D (on the front and back of the elements).

The combination of the measurement results allows for direct conclusions to be drawn on the mechanical behaviour, for example on the forces transmitted via cracks in the concrete.

The first pilot tests were successfully carried out in the summer of 2017.

Compression field models

Cracked membrane model with fixed cracks: General solution, with aggregate interlock

Membrane element

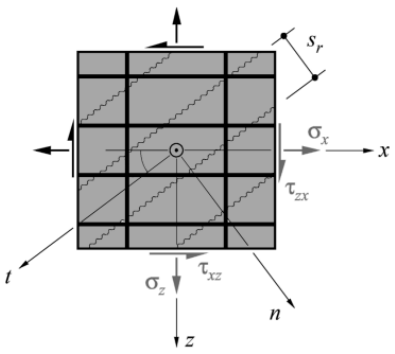

Required material properties:

- Constitutive relationships of concrete and reinforcement
- Bond-slip relationship

Simplified solution method (for given crack inclination and spacing)

Approximate the local variation of the concrete strains $\varepsilon_n^{(c)}$, $\varepsilon_t^{(c)}$, $\gamma_{nt}^{(c)}$ between the cracks based on the TCM

Assumption / estimation of 5 primary unknowns:

- Strains in concrete between two cracks $\{\varepsilon\}^{(c)} = 3$ unknowns)
- Strains due to crack kinematics $\{\varepsilon\}^{(r)} = 2$ unknowns (for known crack direction and distances, $\{\varepsilon\}^{(r)}$ follows from crack opening and crack slip δ_n, δ_t)

Iteration until the following conditions are met (5 equations for 5 unknowns):

- 3 equilibrium conditions at the crack
- 2 aggregate interlock relationships $\sigma_{cnr}(\{\varepsilon\}^{(c)}) = \sigma_{cnr}(\delta_n, \delta_t)$, $\tau_{ctnr}(\{\varepsilon\}^{(c)}) = \tau_{ctnr}(\delta_n, \delta_t)$

Despite the simplification of neglecting the variable concrete strains, the solution is numerically challenging, since the crack interrelationship is highly non-linear and sensitive to small displacements.

It was recently implemented successfully (Gehri 2018) and gives good results.